THERMAL TRANSPORT AND RADIATIVE PROPERTIES OF FIBROUS STRUCTURAL MATERIALS

by

S. J. Lis, R. J. Baschiere, and G. Engholm

General American Transportation Company
MRD Division
7501 Natchez Ave., Niles, Ill.

ABSTRACT

This paper discusses a program in which apparatus were constructed and measurements were made of the thermal transport and radiative properties of various fibrous structural materials.

The thermal conductance apparatus employed a transient technique to measure the thermal conductance of fibrous materials under varying conditions of temperature (200 to 1500°F), environmental pressure (20.2 psia to 0.4 mm Hg), biaxial tension (1 to 109 ppi), and compression (1.9 to 13.7 psi). Based upon the Cenco-Fitch measurements of Mylar film and asbestos paper standards, the thermal conductance apparatus measurements were found to be valid to within 7%. The results of the thermal conductance tests have shown that the presence of a coating on a material does not alter its conductance value. Environmental pressure has been found to affect the conductance values to the extent of causing a twofold increase in the conductance when the pressure is changed from vacuum to an ambient atmospheric pressure.

The thermal emittance apparatus utilized a goniometric technique to spectrally scan the transmitted and reflected radiation from material samples subjected to biaxial tension. Total normal emittance values were calculated from these data. The test data indicated that the magnitude of biaxial tension has no appreciable effect on emittance. The test results also showed that the emittance values, derived at room temperature, can be used in the determination of higher temperature emittance values. A check made to establish the accuracy of the emittance apparatus has shown it to be suitable for the determination of the emittance of both diffuse and specular surfaces to within 29%.

The validity of the temperature measurements obtained from miniature thermocouples woven into the material samples was evaluated. The large variations of temperature (30 to 100°F) which could be found in small areas (1/8 inch diameter) indicated that an estimate of the local temperature could be obtained, but the exact value of the temperature could be established only within 10%. If a "direct method" of total normal emittance were used, the 10% possible error in temperature measurement would result in a 40% possible error in the determination of the emittance value. This result further justifies the use of the "indirect method" of total normal emittance measurement which was used in the program.

NOMENCLATURE

A	surface area
A_r	cross-sectional area of receiver
c_f	specific heat of fabric
c_r	specific heat of receiver
d	deviation from the mean
e	thermocouple emf output
k_f	thermal conductance of fabric
L	thickness of receiver
m_r	mass of receiver
N	number of data used to determine the mean value
P.E.	probable error of the mean
$\dot{Q}$	rate of radiant energy
$\dot{Q}''$	radiation energy per unit area
q_L''	receiver heat loss per unit area
r	radius of hemisphere
t	time
T	absolute temperature
T_H	constant source temperature
T_o	initial receiver temperature
T_r	receiver temperature at time t
$(\frac{\partial T}{\partial x})_f$	temperature gradient in the fabric
$(\frac{\partial T}{\partial \tau})_r$	rate of receiver temperature change

W	weight per unit area
X	thickness of fabric
α	absorptance
α_T	thermal diffusivity
β	proportionality constant
ϵ	total hemispherical emittance
ϵ_λ	spectral hemispherical emittance
κ	slope
λ	wavelength
ρ	reflectance
ρ_f	density of fabric
ρ_r	density of receiver
σ	Stefan-Boltzmann radiation constant
ϕ	elevation angle measured from normal to surface
ψ	azimuth angle

Subscripts

bb	blackbody
i	data point
I	incident
α	absorbed
λ	spectral
ρ	reflected
τ	transmitted

INTRODUCTION

Background

With the advent of aerospace missions, the necessity of developing devices which will enable an aerospace vehicle to traverse the atmosphere upon reentry without undergoing adverse heating effects has become quite apparent. One of these would be the deployment of a fabric decelerator to increase the drag of the vehicle system and, by reducing its velocity, reduce the heating effects. These same factors which cause the vehicle to become heated will act upon the decelerator.

Whereas, most of the heat is transferred to the decelerator by convection, radiation is the mechanism by which the heat will be dissipated by the high temperature, aerodynamic decelerator. Radiation plays an increasingly important role in heat transfer as the temperature of the hot body increases. The degree of temperature rise on the surface as well as within the decelerator is controlled by its ability to diffuse the convective heat input. The mechanism of thermal conduction and, in particular, the thermal diffusivity properties of the material which is deduced from thermal conductance, density, and specific heat properties of the material, are closely inter-related and involved in heating problems of high speed aerodynamic decelerators (see Reference 1). Therefore, the major areas of concern here are (1) the aerodynamic heating rate input, (2) the degree of heat diffused, and (3) the rate at which heat is dissipated, principally by radiation.

The various facets of aerodynamic heat input are heavily dependent upon trajectory, decelerator geometry, and local atmospheric properties. It is therefore futile to generalize aerodynamic heating rates universally applicable to all cases. However, this is not true in the case of basic material thermal properties which are generally applicable but in most cases are not available. The required material properties are the thermal conductance, which is the basic unknown property used to determine the thermal diffusivity of the material, and the total hemispherical emittance, both as they are affected by temperature, ambient pressure, and biaxial tensile and compressive loading.

Objective and Scope

The objectives of the present investigation were to determine experimentally the thermal conductance and total hemispherical emittances of the following fibrous structural materials.

1. Two Nylon fabrics, 1-N and 11-N
2. Three types of HT-1 fabric, (an organic fiber cloth) Type I, Type II, and Type III. **Type I is similar to MiL-C-7350, Type II is similar to MiL-C-7350, Type III is similar to MiL-C-8021.**

3. Fiberglass cloth

4. Fiberglass cloth, aluminum coated

5. Graphite cloth

6. Vitreous silica cloth, uncoated

7. Vitreous silica cloth, TRV 60 coated

8. Vitreous silica cloth, Parson's optical black coated

9. Rene 41, uncoated

10. Rene 41, CS 105 coated

11. Pluton cloth

The scope of this program was to (1) develop an apparatus to determine the thermal conductance of textile materials, normal to the surface, as a function of temperature, ambient pressure, compressive load, and biaxial tensile load, (2) develop an apparatus to determine the total hemispherical emittance of these materials, (3) measurement of the thermal conductance and total hemispherical emittance of the fibrous structural materials, (4) investigate the possibility of attaching miniature temperature transducers to the materials tested and evaluate the accuracy of the transducer in measuring the material's temperature.

Method

Under a previous contract (AF 33(616)-6673) MRD developed an apparatus for measuring thermal conductance of fibrous materials. This work utilized a comparative technique using a material of known conductance and measuring the temperature profiles through composites of known and unknown material was not feasible for application over the extended range. Consequently, a calorimetric technique was developed and found to be successfully adaptable to the type of materials tested. The data from the thermal conductance apparatus were reduced according to an analytical procedure developed herein where the raw data is corrected to produce data linearity and a scheme of root-mean-square fits for the data is used to determine the slope. Since the thermal conductance is inversely proportional to the slope, it is easily determined. The specific heat is primarily a function of the solid constituent fiber. The weight per unit area is considered to be invariant with tensile and compressive loading. Therefore, the thermal diffusivity of the material follows from measured thermal conductance and thickness under load data together with independently determined specific heat and weight per unit area information.

An apparatus was constructed which utilized a goniometric technique to determine the spectral normal emittance of material samples. An investigation was made of the effects of elevated temperature upon several physical characteristics of these samples. This study allowed data to be collected with the materials at room temperature. By placing these results into a computational scheme, the values of total normal emittance were obtained which are applicable to the materials when they are at elevated temperatures.

Another apparatus was developed to establish the temperature measuring accuracy of miniature thermocouples woven into the materials. This apparatus permitted the temperature measurements of convectively heated materials to be accomplished simultaneously by the embedded thermocouple and a radiation pyrometer. A comparison of the temperatures determined by these two devices provided an indication of the accuracy of the thermocouple readings.

THERMAL CONDUCTANCE

Textile materials are not homogeneous. When a temperature potential is developed across such a material, normal to the surface, heat is transferred by conduction, convection, and radiation through the interstitial gas. When speaking of the thermal conductivity of such a material, therefore, what is meant is the effective thermal conductivity which occurs as a result of these various modes of heat transfer. This compound property as used throughout this paper, is termed the thermal conductance of the fibrous structural material. Furthermore, the thermal conductance as measured and reported herein is in the direction normal to the surface of the fabric. The thermal conductance along the fibers and parallel to the fibrous structural material is quite different from the values reported herein. This fact is self-evident when the structure of the material is considered in both the normal and parallel direction. Thus, the thermal conductance of the fibrous structural material shows this type of material to be anisotropic as well as inhomogeneous.

Transient Calorimetric Technique

The technique of measuring thermal conductance of fibrous materials by the steady state, comparative technique, i.e., by using a heat meter of known materials (as was reported in Reference 2), was abandoned in favor of a transient calorimetric technique. The primary reason for this is to avoid the interface warpage problem that exists when a composite heat meter is subjected to temperature gradients. Furthermore, to achieve accurate temperature differences across a suitable heat meter material, the material would of necessity be of very low thermal conductivity (of the order of the insulating material surrounding the heat meter system) or would require thicknesses beyond which unidirectional heat transfer assumptions are valid.

The calorimetric technique used in the present application requires only two functional components, a source and a receiver. Figure 1 shows the arrangement for the device used. The source elevates and maintains the temperature of the test sample at a desired level. The receiver is brought down into contact with the hot test sample to begin the test run. The thermal conductance of the sample is then determined from the temperature-time history of the receiver.

The basic theory involved in such a system is described by the following heat balance at the fabric-receiver interface.

Heat conducted through the fabric equals the heat stored in the receiver, plus the heat losses, namely:

$$-k_f A_r \left(\frac{\partial T}{\partial x}\right)_f = m_r c_r \left(\frac{\partial T}{\partial t}\right)_r + q_L \qquad (1)$$

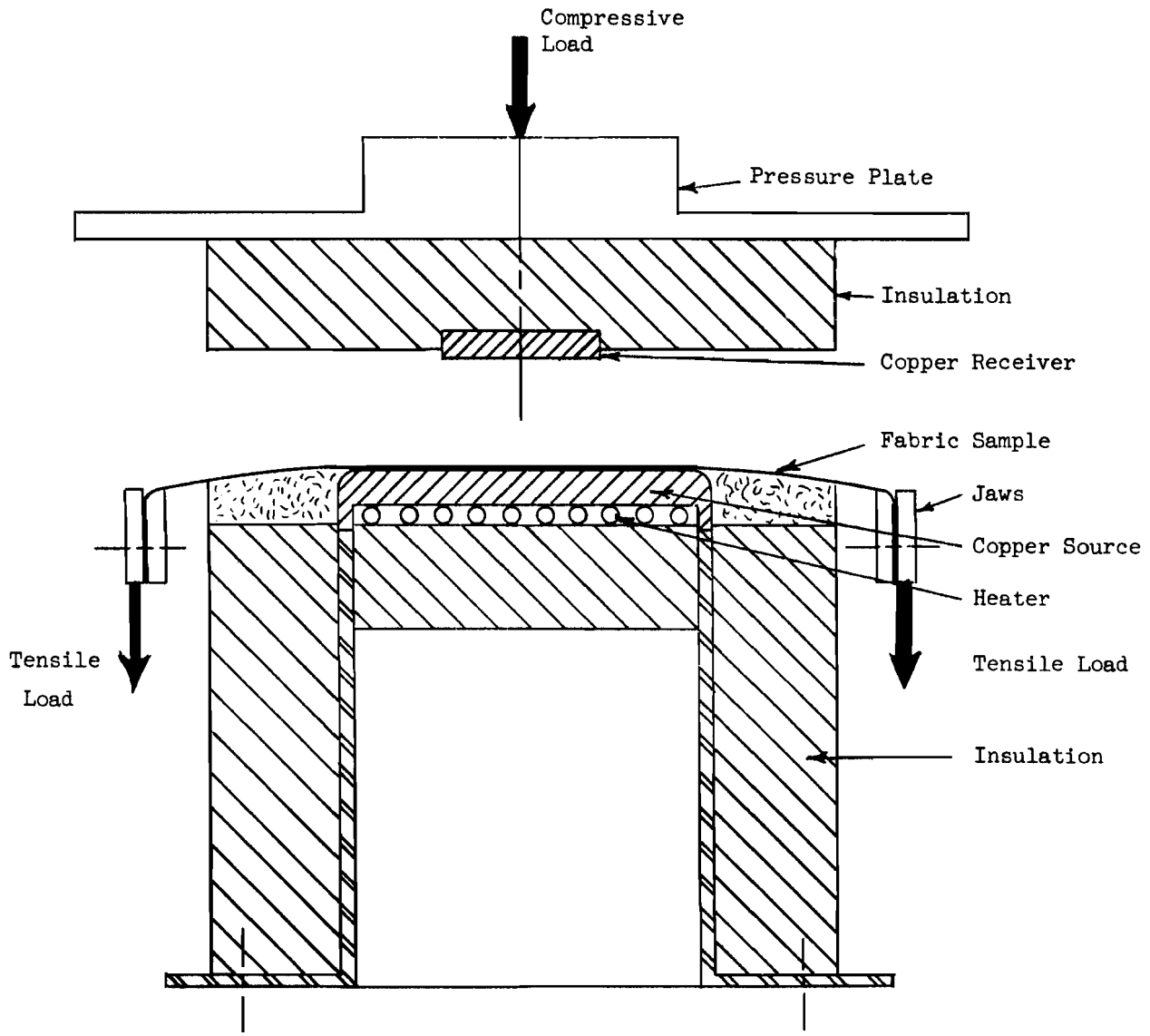

Figure 1 SKETCH OF COLORIMETRIC TECHNIQUE

If heat losses are neglected the heat balance equation can be reduced to:

$$-k_f A_r \left(\frac{\partial T}{\partial x}\right)_f = m_r c_r \left(\frac{\partial T}{\partial t}\right)_r \tag{2}$$

Furthermore, if the source temperature is maintained constant and the receiver is a good conducting, high diffusivity material such as copper, the heat balance then can be described as:

$$k_f A_r \frac{T_H - T_r}{X} = m_r c_r \frac{dT_r}{dt} = \rho_r A_r L c_r \frac{dT_r}{dt}$$

or

$$\frac{dT_r}{dt} + \frac{k_f}{\rho_r c_r L X} T_r = \frac{k_f}{\rho_r c_r L X} T_H \tag{3}$$

The integral solution of this equation is:

$$t = \frac{\rho_r c_r L X}{k_f} \ln \left[\frac{T_H - T_o}{T_H - T_r} \right] \tag{4}$$

From the form of Equation (4) it can be seen that a plot of time, t, versus the logarithm of temperature difference will be linear and that the slope is inversely proportional to the thermal conductance of the fabric sample. The temperature time data of the receiver may thus be reduced to yield the thermal conductance of the fabric sample.

The following assumptions were made to obtain Equation (4).

(a) Negligible heat losses from the receiver

(b) Rapid response temperature measurement

(c) Constant source temperature

(d) Uniform temperatures within the receiver.

The effect of heat losses would show itself in the data as a curvalinear plot of the time versus logarithm of temperature difference. These losses are very difficult to measure accurately, but with proper insulation they should be small. If heat losses are included and these heat losses are assumed to be constant during the test run, then a heat balance at the fabric-receiver interface becomes:

$$k_f \frac{T_H - T_r}{X} = \rho_r c_r L \frac{dT_r}{dt} + q_L'' \tag{5}$$

The solution for Equation (5) is :

$$t = \frac{\rho_r c_r LX}{k_f} \ln \left[\frac{T_H - T_o - \frac{q_L'' X}{k_f}}{T_H - T_r - \frac{q_L'' X}{k_f}} \right] \tag{6}$$

where T_o is the temperature of the receiver at time $t = t_o = 0$.

The effect of including the heat loss is seen to appear as a correction for the temperature difference as monitored during a test run. The conductance, k_f, will not vary greatly during the test run, consequently the correction terms can be considered as a constant, say:

$$Q_L = \frac{q_L'' X}{k_f} \tag{7}$$

The millivolt response for temperature difference may be related for a linear responding thermocouple as:

$$e = \beta(T_H - T_r) \tag{8}$$

Thus Equation (6) may be written as

$$t = \frac{\rho_r c_r LX}{k_f} \ln \left[\frac{e_o - Q_L'}{e - Q_L'} \right] \tag{9}$$

where

$$Q_L' = \beta Q_L = \frac{\beta q_L'' X}{k_f} \tag{10}$$

Consider a time period $t_i < t_{i+1} < t_{i+2}$ taken at equal increments and the corresponding emf (Temperature difference) readings $e_i > e_{i+1} > e_{i+2}$. The Equations (9) which apply at time t_{i+1} and t_{i+2} are

$$t_{i+1} - t_i = \frac{\rho_r c_r LX}{k_f} \ln \left[\frac{e_i - Q_L'}{e_{i+1} - Q_L'} \right]$$

and (11)

$$t_{i+2} - t_i = \frac{\rho_r c_r LX}{k_f} \ln \left[\frac{e_i - Q_L'}{e_{i+2} - Q_L'} \right]$$

Taking a ratio of Equations (11) yields

$$\frac{t_{i+1} - t_i}{t_{i+2} - t_i} = \frac{1}{2} = \frac{\ln\left[\frac{e_i - Q_L'}{e_{i+1} - Q_L'}\right]}{\ln\left[\frac{e_i - Q_L'}{e_{i+2} - Q_L'}\right]} \tag{12}$$

Cross multiplying and exponentiating yields the expression for Q_L' as:

$$Q_L' = \frac{e_i\, e_{i+2} - e_{i+1}^2}{e_{i+2} + e_i - 2e_{i+1}} \tag{13}$$

Thus it is seen that for each set of data points: i, i+1, and i+2 a value of Q_L' may be determined.

Returning to Equation (9) it is instructive to examine the temperature difference (emf) of a test run as time approaches infinity. Solving Equation (9) for the emf, (e) occurring at time, t, such that $e = e_o$ at some initial time $t = 0$, results in:

$$e = Q_L' + \exp\left(-\frac{k_f t}{\rho_r c_r L X}\right)(e_o - Q_L') \tag{14}$$

taking the limit:

$$\lim_{t \to \infty} e = Q_L' \tag{15}$$

Therefore, the heat loss correction, Q_L', determined by successive points during the run by Equation (13) corresponds to the heat loss correction approached as time increases.

Thermal Conductance Apparatus

The steady state thermal conductance apparatus originally built on Contract AF 33(616)-6673* was modified to permit use of the transient, calorimetric technique and the resulting system is illustrated in Figure 2.

* WADD TR 60-670 pt II

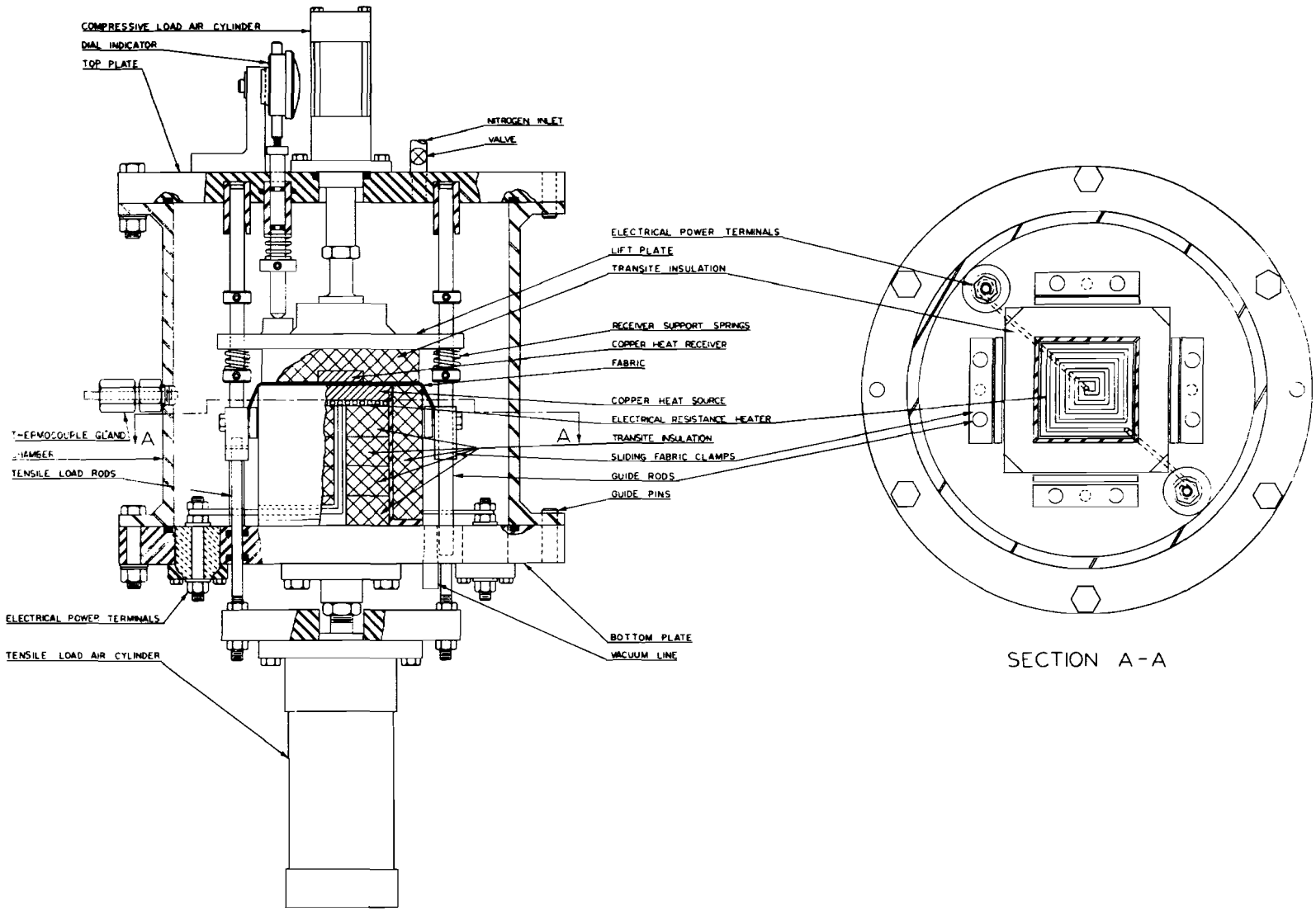

Figure 2 THERMAL CONDUCTANCE APPARATUS

The interior of the heater chamber was flame sprayed with aluminum oxide to form a 0.010-inch thick coating which is thick enough for electrical insulation yet thin enough to minimize the temperature difference between the copper source plate and the heater coils. A flat heater was wound from B&S No. 10 gage Kanthal A-1 wire and mounted in good thermal contact with the underside of the copper source plate. To assure good contact Cerafelt* (a flexible, high temperature felt insulation) was placed between the heater support and the heater windings. The entire heat source assembly is surrounded by Transite* insulation. The test fabric is held in four movable jaws, one on either side of the heater assembly. Thus when a tensile load is applied equally to the four movable jaws, the fabric sample is stretched over the hot plate in biaxial tension.

The receiver is an electrolytically pure copper "button", 1.497 inch diameter and 0.375 inch thick. It is held securely within Marinite* 36 insulation by Sauerisen ceramic cement. The well, machined into the supporting insulation, is made such that the receiver protrudes approximately 1/16 inch beyond the flush position to assure that only the receiver is in contact with the test fabric sample. A miniature chromel-constantan thermocouple** was located in the receiver so that its insulated junction is within 1/8 inch of the geometric center of the receiver. The source temperature was measured by a similar thermocouple located 1/4 inch from the surface of the copper source plate. Both thermocouples were of the silver sheathed type to minimize thermal disturbance due to local conductivity differences.

The receiver assembly (copper receiver and surrounding insulation) was bolted to the pressure plate and supported by four springs which hold the assembly removed from the test sample until the desired temperature level is reached.

The size of the receiver and the receiver material are important in the technique. By using copper, uniformity of temperature within the receiver is maximized. If the receiver is too large thermal gradients will exist within the material due to finite times available for thermal diffusion, even in copper. If the receiver is too small the receiver will respond to the high temperature too rapidly so that the measuring instrument as well as the test fabric would not respond without significant lag. The present receiver design was found to be a compromise between these limits.

The technique requires transient measurements of source and receiver temperatures. It is necessary that the thermocouple readout equipment respond fast enough to follow these transients. A CEC recording oscillograph was initially utilized to measure and record the thermocouple responses. This

* Johns Manville Co.
** Baldwin-Lima-Hamilton Co., Type TCRC-LAG

instrument is capable of recording with response times in the order of milliseconds. This approaches the response times of the thermocouples used. It was found, however, that these rapid response times were not necessary and that more accuracy in recording was gained by using a recording potentiometer.*

It is important to maintain a constant source temperature. This can be accomplished by (1) having a large thermal mass for a source so that the heat transferred to the receiver would have a negligible affect on the source temperature, or (2) by controlling the heater power to make up heat transferred to the receiver. The merits of both these methods were studied and the best approach was determined to be heater power regulation.

The control system consists of a proportioning controller**. The source temperature to be regulated is continuously monitored by a second thermocouple within the copper source plate which sends a signal to the controller. As the thermocouple approaches the set control point a switch within the controller is actuated which controls an external relay. The external relay is part of the heater power circuit and is so wired that the heater is connected to either the high power or the low power tap of a variable autotransformer (Variac). Figure 3 is a sketch of the heater control circuit. The controller allows high power to the heater until the set point is approached, at which time the controller switch actuates the relay and causes a step-down in power. The voltage ratio between the high and low setting is approximately 1.2. In addition, the circuitry for the temperature controller was modified to extend its range from 1000°F to beyond the 1500°F limit for the test materials.

The thermal conductance apparatus (TCA) is shown in Figures 4 and 5.

Thickness Determination

The compressometer shown in Figures 6 and 7 was used to determine fabric thickness as a function of compressive load. In order to eliminate an uneven load distribution the force was applied to a ground and polished surface by suspending weights at the end of a .020-inch diameter piano wire secured at the centroid of block A (see Figure 6). The fabric was placed over a small hole in a ground steel plate, and the wire was passed through the cloth and steel plate until block A came to bear on the material. The initial thickness was measured under load of 3 ounces per square inch (the weight of the block alone). Weights were then applied to the wire and subsequent deflections were noted by a dial indicator mounted on the ground plate adjacent to block A. The maximum probable error in the initial thickness is 0.00003-inch or 0.55%. The stress vs. strain relationships for all the fabrics were determined in this manner.

* Leeds & Northrup AZAR Strip Recorder.
** West Instrument Model JPS-22

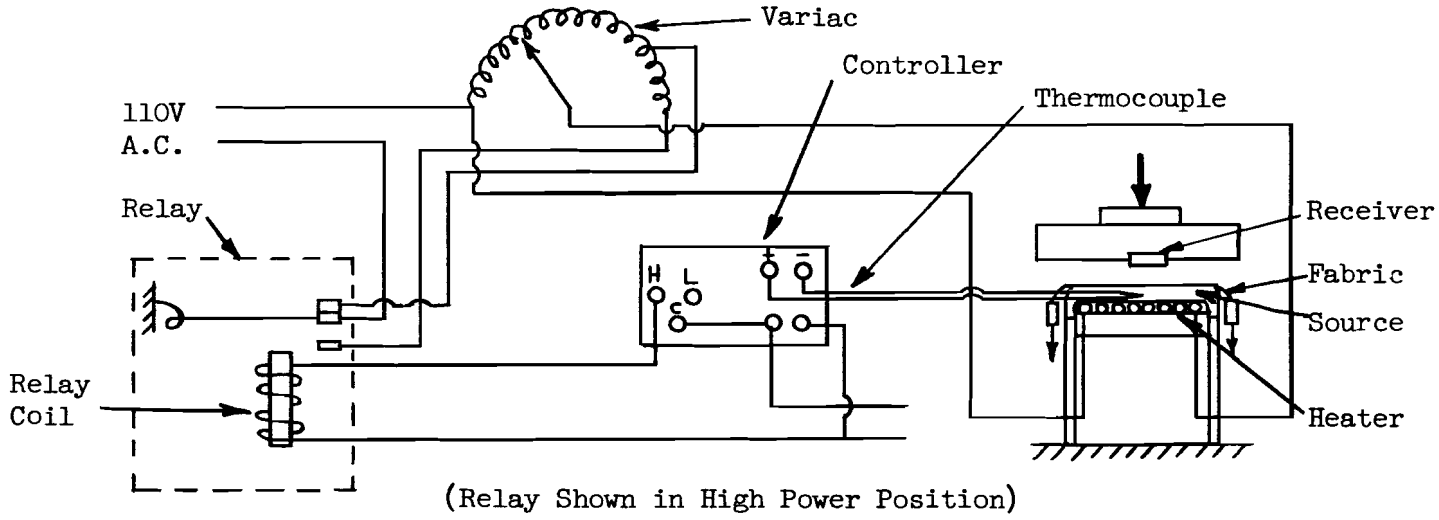

Figure 3 THERMAL CONDUCTANCE APPARATUS HEATER CONTROL CIRCUIT

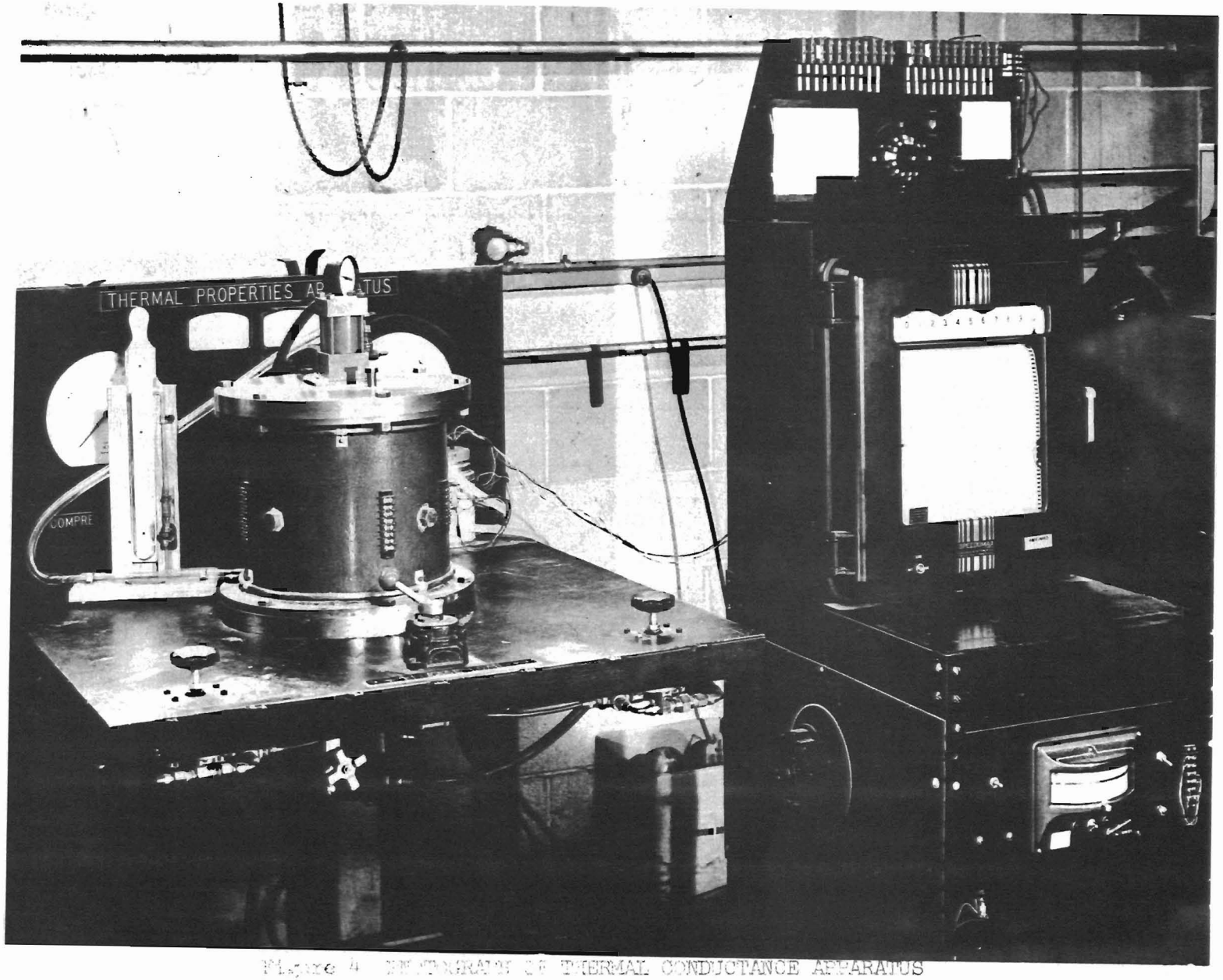

Plate 4 PHOTOGRAPH OF THERMAL CONDUCTANCE APPARATUS

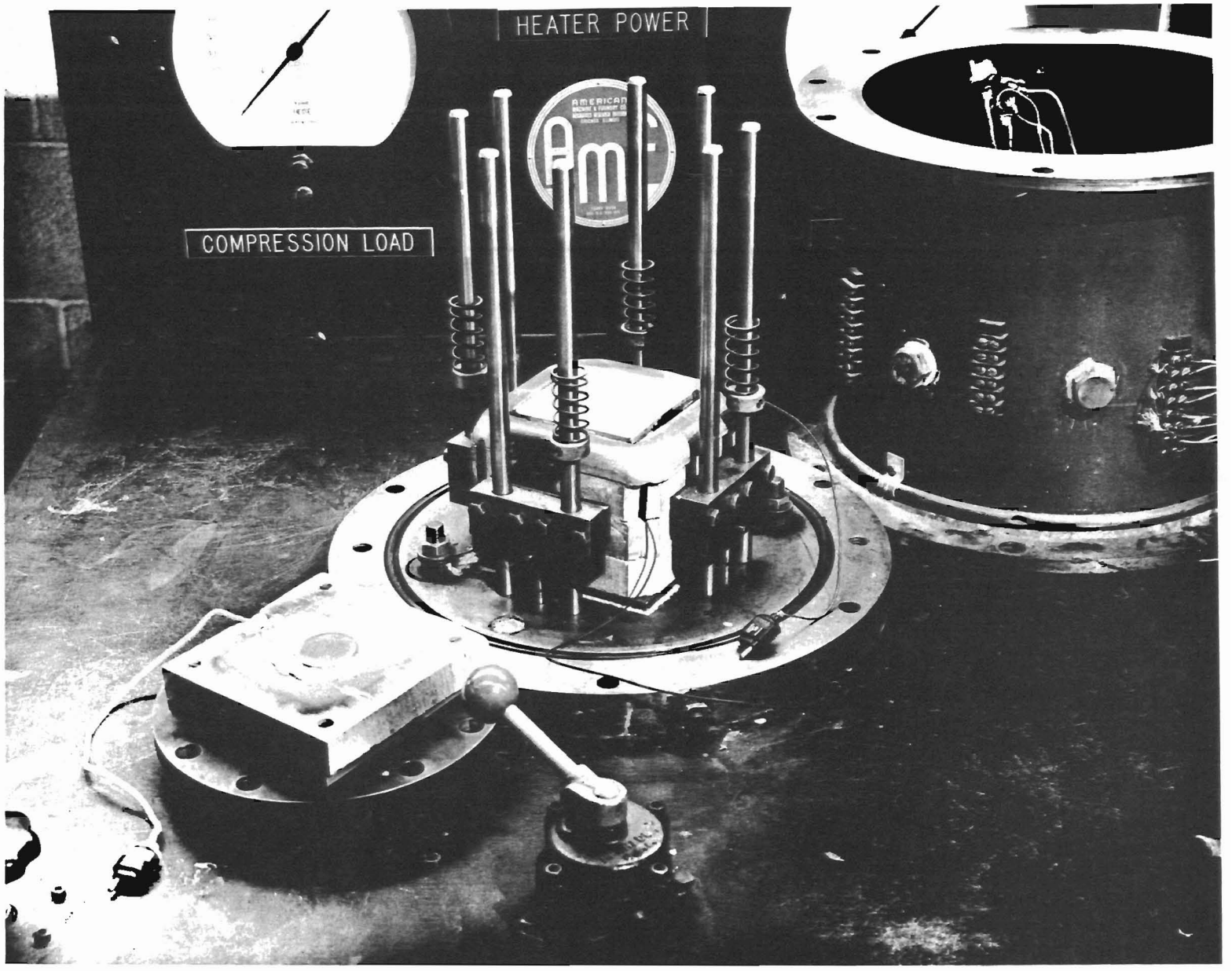

Figure 5 PHOTOGRAPH OF HEAT SOURCE AND RECEIVER

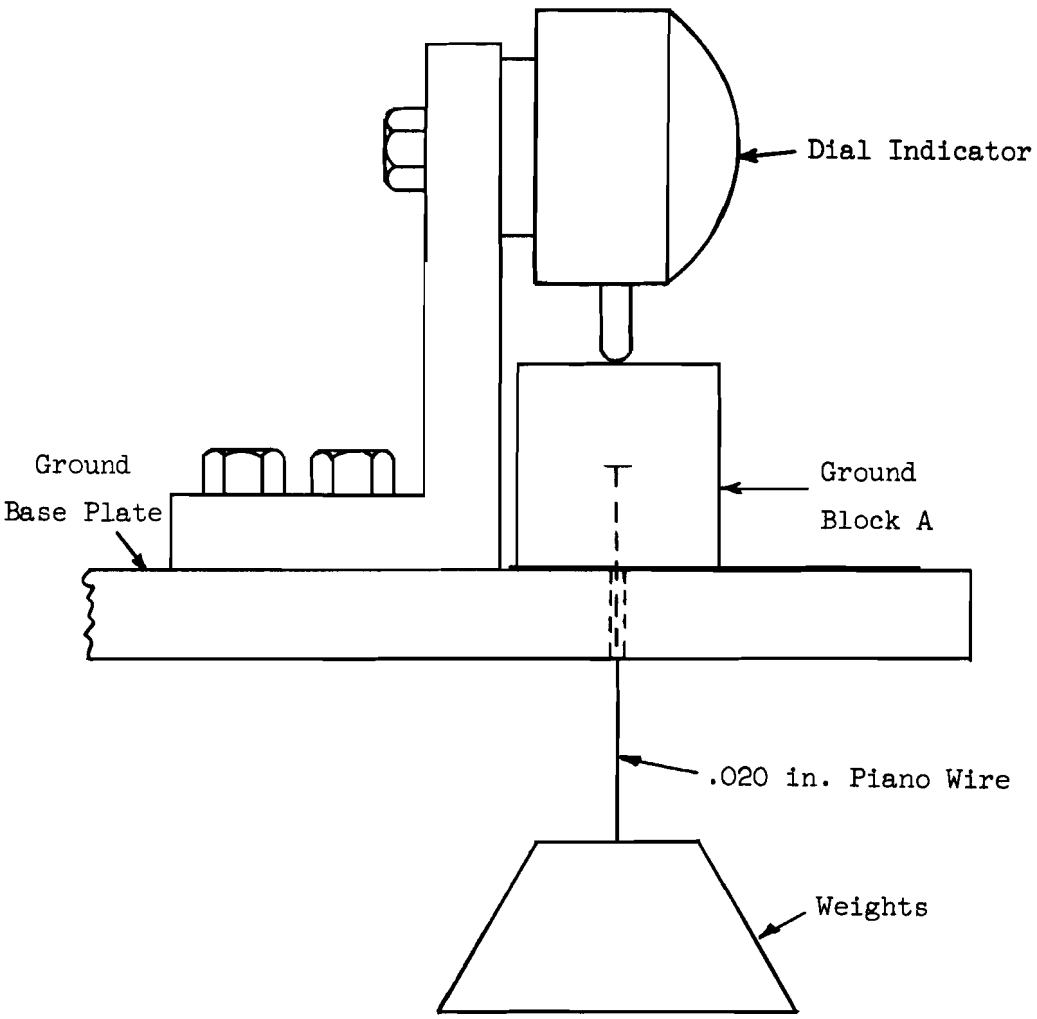

Figure 6 SKETCH OF COMPRESSOMETER

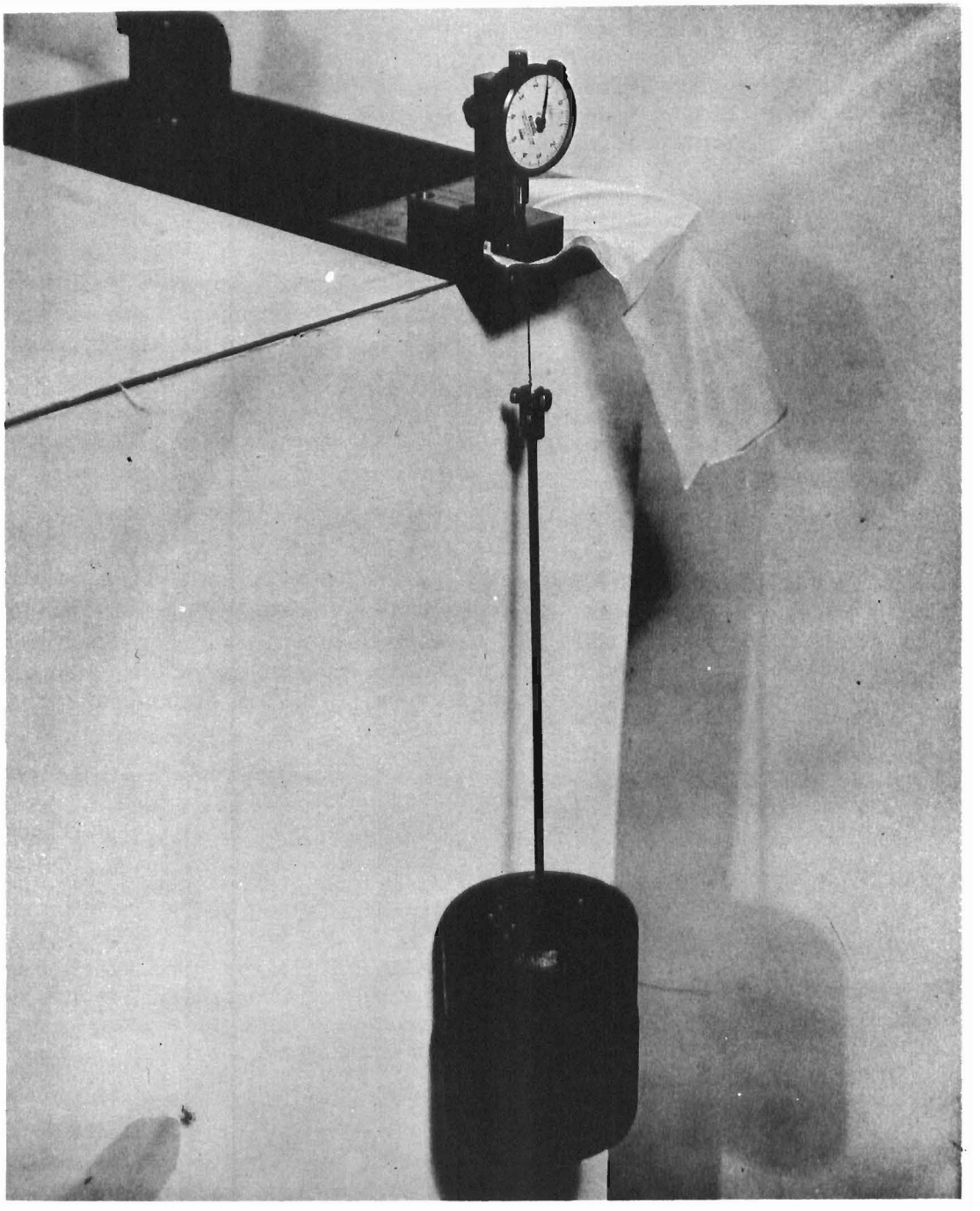

Figure 7 PHOTOGRAPH OF COMPRESSOMETER

Method of Data Reduction

The thermal conductance apparatus data consists of a recording potentiometer strip chart trace of copper heat source temperature and copper heat receiver temperature. To reduce the conductance data, the thermocouple emfs for source and receiver are read from the strip chart at equal intervals of time (in most cases, every minute) and the temperature (emf) difference is computed. A typical set of raw data is illustrated in Figure 8. As can be seen the raw data are not quite linear. For each successive increment of time the heat loss correction is determined by Equation (13). The arithmetic average is computed of the heat loss corrections. The average correction is applied to the raw set of data.

Applying such a correction term to the raw data illustrated in Figure 8 it is seen that the data is indeed linearized. The fabric conductance is proportional to the slope of this line, consequently the conductance is easily deduced. This is accomplished by applying the method of least squares to the corrected data and determining the best fit line and its corresponding slope. The thermal conductance of the fabric sample is therefore:

$$k_f = (\rho_r c_r LX) \cdot \kappa \tag{16}$$

The data reduction for all the materials tested over the range of variables considered is a tedious task if done manually, therefore, data reduction computations were programmed into the IBM 1620 computer and the raw data were fed to the computer. Noting the manner in which the thermal conductance is determined the best fit slope is calculated relative to each data point during the test run. The average conductance determined from this procedure represents a finite deviation from each data point. The probable error, P.E., of the average therefore may be determined statistically from the relation:

$$\text{P.E.} = \frac{0.8453\ \Sigma d}{N\sqrt{N-1}} \tag{17}$$

The probable error for the individual thermal conductance values is a measure of the fit to linearity of the data for each particular run.

Three test runs were made for each condition tested. The average thermal conductance for these repetitions were computed and the probable error of the mean determined in a similar manner. The probable error of average thermal conductance values is a measure of the reproducibility of the runs and therefore a measure of reliability and accuracy.

Calibration Tests

The Thermal Conductivity Apparatus (TCA) has been designed to handle thin, flexible specimens of low thermal conductivity. If a rigid specimen is tested it will not be able to conform to the source and receiver surfaces and the test

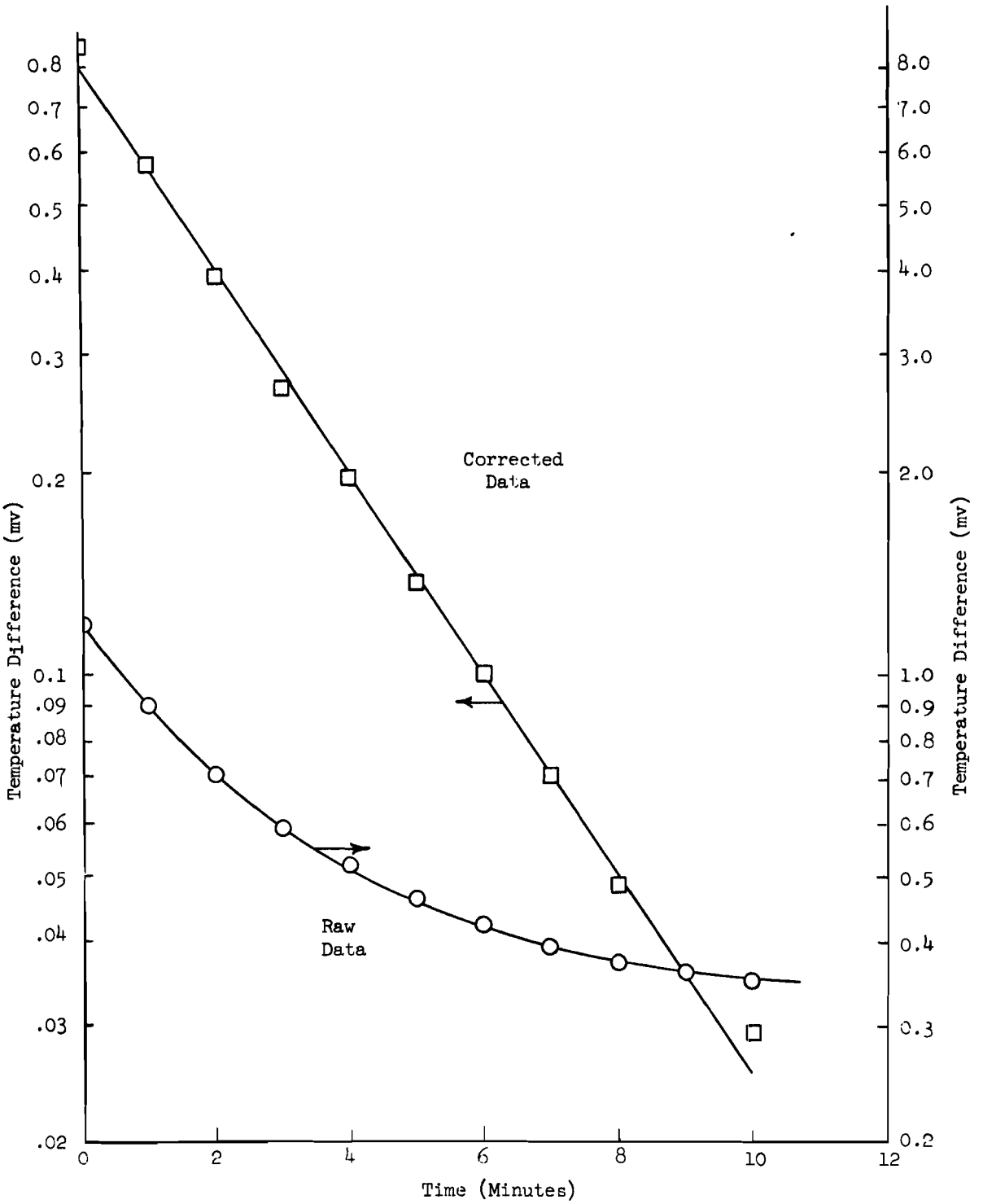

Figure 8 TEST RUN FOR HT-1 TYPE I

data will result in computed thermal conductances that are too low since only a portion of the specimen area will be able to conduct heat properly.

Several materials were collected from outside suppliers for which thermal conductance had been measured. These materials and their suppliers are:

Asbestos Paper	Johns-Manville Corp.
Mylar Film	E. I. DuPont de Nemours & Co.
Teflon Film	E. I. DuPont de Nemours & Co.
27U-7-7GM Graphite	Great Lakes Carbon Corp.

The thermal conductance of each of these materials was measured in the thermal conductance apparatus. Asbestos paper specimens meet the requirements of the TCA. The data reported by Johns-Manville Corp show that the previous thermal history can affect the conductance of their asbestos paper by as much as 44%. The manufacturing variations can result in even larger differences of conductivity between various samples of the same material. The samples tested in the TCA were also tested in a Cenco-Fitch apparatus to obtain a second source of thermal conductivity data for comparison. The asbestos paper data compare to within 6%. Mylar film was also used for comparisons, the Cenco-Fitch and TCA data agree to within 7%.

Measured Teflon film conductance did not agree with reported values. This was attributed to the fact that the sample measured was not uniform but contained slight "pimple type" imperfections which voided certain areas and made its surfaces rough and uneven. The material was rigid enough to prevent the "pimples" from smoothing out under the test conditions.

Further evidence of validity is supplied by a comparison of thermal conductance of 1N Nylon material. In Reference 2 the thermal conductance was measured by two independent methods i.e., by the Cenco-Fitch method and the comparative technique on the Thermal Properties Apparatus (TPA). These data show good agreement with the average thermal conductance values obtained with the calorimetric technique utilized in the present thermal conductance apparatus.

The problem of selecting thermal conductance standards is at least as difficult as that of selecting a technique for measuring thermal conductance. The apparatus developed has been designed for fabric specimens and is suited to measurement of thin, flexible, low conductance materials. Thus, the "standard" used to calibrate the apparatus must also be thin, flexible and of low conductance. The "standard" then must also be stable, that is its conductance must not vary from test to test due to thermal or humidity effects. Mylar film appears to best meet these requirements. Based upon the Cenco-Fitch measurements, the TCA measurements are valid to within 7%.

Thermal Diffusivity

The thermal diffusivity is defined as:

$$\alpha_T = \frac{k_f}{\rho_f c_f} \tag{18}$$

The thermal conductance has been measured. In order to determine the thermal diffusivity, the density and specific heat of the material must also be known.

If it is assumed that the weight per unit area of the fibrous structural materials is not significantly changed by the imposed biaxial and compressive stresses, then the density varies as the thickness of the material under load, that is:

$$\rho_f = \frac{W}{X} \tag{19}$$

The weight per unit area data for all the materials have been collected from manufacturer's data and/or measured by means of a precision analytical balance. The thickness under load of the fabric materials has also been measured during the course of this program by the compressometer technique developed. This technique was used to obtain the fabric densities.

It has been shown (Reference 2) that the specific heat of a fabric material is closely approximated by the specific heat of the constituent fiber's solid material. This fact has been utilized in evaluating the specific heat information obtained from the suppliers for the fabrics tested. The thermal diffusivities of the materials were computed from average thermal conductance data and from the collected and/or measured data for density and specific heat.

THERMAL EMITTANCE

Method of Approach

The Stefan-Boltzman law gives the rate of energy, $\dot{Q}$, radiated from a surface as:

$$\dot{Q} = \epsilon \sigma A T^4 \tag{20}$$

where ϵ, is the total hemispherical emittance of the surface.

Total hemispherical emittance is defined as the sum of all the radiation for all wavelengths emitted from any element of a surface over the entire solid angle of a hemisphere. It is the efficiency of the surface as a radiator of thermal energy. A surface which emits the theoretical maximum amount of energy is termed a "blackbody" and has an ϵ of unity.

The spectral hemispherical emittance, ϵ_λ, is the emittance of an element of a surface over the entire solid angle of a hemisphere for a specific wavelength. If ϵ_λ is invariant with wavelength, the surface is defined as a "greybody". The greybody values of ϵ_λ are thus a fixed percentage of those of a blackbody.

Most materials are neither "black" nor "grey" bodies but possess ϵ_λ values which vary with wavelength. (Reference 3)

The spectral emittance values of a material are a function of the physical characteristics of the exposed surface of the material. As the material's temperature is increased, the characteristics of this surface may change. Therefore, the spectral emittance values can be a function of temperature.

Another factor which could alter the spectral emittance values of a material are changes in the geometry of the surface of the material. This could be a large effect for the woven materials considered in this study. Due to the nature of the weave, there is a percentage of the surface area which presents no obstacle to the passage of energy through the material. As a woven material is loaded in biaxial tension, the strands are displaced and/or their cross-sectional areas altered. This changes the percentage of open area and thus the radiant properties.

Direct Method

From equation (20), the total hemispherical emittance ϵ is given by

$$\epsilon = \frac{\dot{Q}}{\sigma A T^4} \tag{21}$$

which permits an experimental evaluation of ϵ based upon a measurement of the radiant flux, $\dot{Q}/A$, leaving the body and a measurement of the temperature of the body. In practice, the direct evaluation is obtained by comparing the material with a blackbody emitter.

Theoretically, a cavity having an infinitesimal opening emits blackbody radiation through its opening when the inner surfaces of the cavity are at a uniform temperature (Reference 4). Actually, it is not too difficult to prepare such a blackbody in the laboratory which can attain an emittance as high as 0.9999 (Reference 5). Such a blackbody radiative source is a standard of comparison against which the rate of emission of a surface of unknown ϵ can be measured.

Denoting the blackbody by subscript bb, the ratio of the emittance of the blackbody and an unknown surface is obtained from equation (21) as

$$\frac{\epsilon}{\epsilon_{bb}} = \frac{\dot{Q}}{\dot{Q}_{bb}} \frac{T_{bb}^4 A_{bb}}{T^4 A} \tag{22}$$

Equation (22) may be simplified if the following conditions and assumptions are introduced.

1. ϵ_{bb} is unity.
2. Equal areas of the unknown surface A and the blackbody surface surface A_{bb} are observed at equal distances, r.
3. Evaluate $\dot{Q}$ by the following relationship (Reference 6) which expresses the rate of emission $\dot{Q}$ in terms of the radiation flux $\dot{Q}''$, at a constant distance, r, from the emitting surface as

$$\dot{Q} = r^2 \int_{\phi=0}^{\phi=\frac{\pi}{2}} \int_{\psi=0}^{\psi=2\pi} \dot{Q}'' \cdot \sin\phi \; d\phi \, d\psi \tag{23}$$

4. Evaluate $\dot{Q}_{bb}$ by integrating the directional emission at any angle ϕ of the blackbody surface in terms of the normal flux ($\phi = 0$) and Lambert's Law. Thus

$$\dot{Q}_{bb} = r^2 \int_{\phi=0}^{\phi=\frac{\pi}{2}} \int_{\psi=0}^{\psi=2\pi} \dot{Q}''_{bb,\,\text{normal}} \cdot \cos\phi \; \sin\phi \; d\phi \, d\psi \tag{24}$$

5. Maintain the unknown surface and the reference blackbody at the same temperature.

The utilization of the above 5 items permits the solution of Equation (22) in the form:

$$\epsilon = \frac{\int_{\phi=0}^{\phi=\frac{\pi}{2}} \int_{=0}^{\psi=2\pi} \cdot \dot{Q}'' \sin\phi \, d\phi \, d\psi}{\int_{\phi=0}^{\phi=\frac{\pi}{2}} \int_{\psi=0}^{\psi=2\pi} \dot{Q}''_{bb,\,\text{normal}} \cos\phi \sin\phi \, d\phi \, d\psi} \tag{25}$$

The basic difficulty in applying this direct approach to the determination of the total hemispherical emittance of a material is that it is very difficult to measure an accurate temperature of the material. Any error in material temperature will result in a large error in emittance since emittance is proportional to the fourth power of the body's absolute temperature. Since there is no technique available for accurately measuring the temperature of a thin material radiating at high temperature (i.e., hot parachute) it is apparent that the direct approach to emittance determination is of uncertain accuracy.

Indirect Method

When a beam of monochromatic radiation falls upon the textured surface of an inhomogeneous surface such as a woven material, the energy is partly (1) reflected at the surface, (2) reflected by the inhomogeneities within the body of the material, (3) absorbed within the material, and (4) transmitted through the material. For such a substance some of the energy which is reflected has also been partially transmitted (being reflected back by the internal structure). Reflectance and transmittance can be defined only in terms of the energy which emerges from the two respective sides of the sample. Radiation which is neither reflected from nor transmitted through the materials is absorbed. The sum of the transmitted, reflected, and absorbed energies at a given wavelength must be equal to the intensity of the incident energy at the identical wavelength or,

$$\dot{Q}_{I,\lambda} = \dot{Q}_{\rho,\lambda} + \dot{Q}_{\tau,\lambda} + \dot{Q}_{\alpha,\lambda} \tag{26}$$

Dividing Equation (26) by the intensity of the incident monochromatic flux we obtain a relationship between the spectral transmittance, reflectance and absorptance of

$$1 = \rho_\lambda + \tau_\lambda + \alpha_\lambda \tag{27}$$

Using Kirchoff's law;

$$\epsilon_\lambda = \alpha_\lambda \tag{28}$$

and placing Equation (27) into Equation (28), the spectral emittance is defined by

$$\epsilon_\lambda = 1 - (\tau_\lambda + \rho_\lambda) \tag{29}$$

Thus the measurement of spectral emittance can be reduced to a determination of spectral transmittance and reflectance.

The total hemispherical emittance value can be obtained from the spectral emittance data.

$$\epsilon = \frac{\int_0^\infty \epsilon_\lambda \frac{d\dot{Q}''_{bb,\lambda}}{d\lambda} d\lambda}{\int_0^\infty \frac{d\dot{Q}''_{bb}}{d\lambda} d\lambda} \tag{30}$$

The material temperature is required in the computation since $\frac{d\dot{Q}''_{bb}}{d\lambda}$ is given by

$$\frac{d\dot{Q}''_{bb}}{d\lambda} = \frac{2 C_1 \pi}{\lambda^5 (e^{C_1/\lambda T} - 1)} \tag{31}$$

where: $C_1 = 0.18892 \times 10^8$ B-μ^4/hr-ft^2

$C_2 = 25{,}896\mu$ -R

The integrated form of the denominator of Equation (3) is given by

$$\int_0^\infty \frac{d\dot{Q}''_{bb}}{d\lambda} d\lambda = \frac{12 C_1 \pi^5}{90 C_2^4} T^4 = \sigma T^4 \tag{32}$$

Therefore the value of the total hemispherical emittance as given by Equation (30) is seen to be a function of the fourth power of the material's temperature.

The direct and indirect procedures for measuring total hemispherical emittance, ϵ, are both dependent upon the temperature of the material. The difference between the two procedures is the manner in which the temperature affects the experimental results. In the direct procedure, an error in the measurement of the material's temperature is reflected in the evaluation of the blackbody energy rate term, $\dot{Q}_{bb}$, of Equation (22). This directly effects the evaluation of the value of ϵ. In the indirect procedure, the evaluation of the spectral hemispherical emittance, ϵ_λ, is fairly independent of the material

temperature. The temperature of the material is only used to indicate the temperature at which the data were obtained. When total hemispherical emittance is calculated through the use of Equation (30), temperature must be introduced. The temperature that is introduced is the value for which the emittance value is desired. Since spectral emittance is known to be a weak function of temperature, one set of spectral emittance data can be used over a range of temperatures. If the temperature for which emittance data is desired falls within the region of applicability of the available spectral emittance data, a value of ϵ, can be obtained. With this procedure, the material temperature at which the data was taken is only used as a reference condition.

Since an accurate direct measurement of the elevated temperature of the material tested can not be achieved through presently known techniques, the approach which is least affected by material temperature was adopted. Therefore, the indirect approach was used to obtain the data presented in this report.

Experimental Apparatus

As previously detailed, if all of the energy incident upon a material, $Q_{I,\lambda}$ reflected from a material, $Q_{\rho,\lambda}$ and transmitted from a material, $Q_{\tau,\lambda}$ are known, the spectral hemispherical emittance, ϵ_λ, can be found. The technique used to obtain these values was suggested by the work of Clark, Vinegar, and Hardy (Reference 7). In their system, a test sample is exposed to a beam of normally incident energy. While the sample is exposed to the beam, a detector measures the energy propagating from the sample in all directions. During the energy measurement, the detector is maintained at a fixed distance from the sample and is rotated hemispherically around the sample. After the scanning is completed, the sample is removed and the incident energy beam is scanned in the same manner. With the appropriate integration of these results, values of $\dot{Q}_{\rho,\lambda}$, $\dot{Q}_{\tau,\lambda}$ and $\dot{Q}_{I,\lambda}$ can be obtained. The emittance apparatus constructed for this program employed this same procedure.

This incident energy for the apparatus was furnished by an electrically heated silicon bonded carbide rod (Globar). A Perkin-Elmer 99 monochromator with an evacuated thermocouple was used to measure the spectral radiation. The use of a NaCl prism, NaCl entrance window, and CsBr window for the thermocouple, permitted measurements over the wavelength range from 2 to 15 microns. This wavelength range accounts for 73% of the energy emanating from the 2200°F Globar source. Because of the size and sensitivity of the monochromator, the sample is rotated with respect to the monochromator to obtain the necessary scanning.

The sample (in the form of a 4 x 4-inch square) was mounted in the fixture shown in Figure 9. The fixture was designed so that the sample could be viewed continuously up to 5° from the plane of the material. When the sample was held in the fixture, it was subjected to a force of biaxial tension. The biaxial loading of the specimen was accomplished by means of four threaded screws coupled to four Dillan load cells (see Figure 10). The load cells are capable of producing tensile loads of up to 100 pounds. The prevailing tensile load is read directly from calibrated dial gages on the load cells.

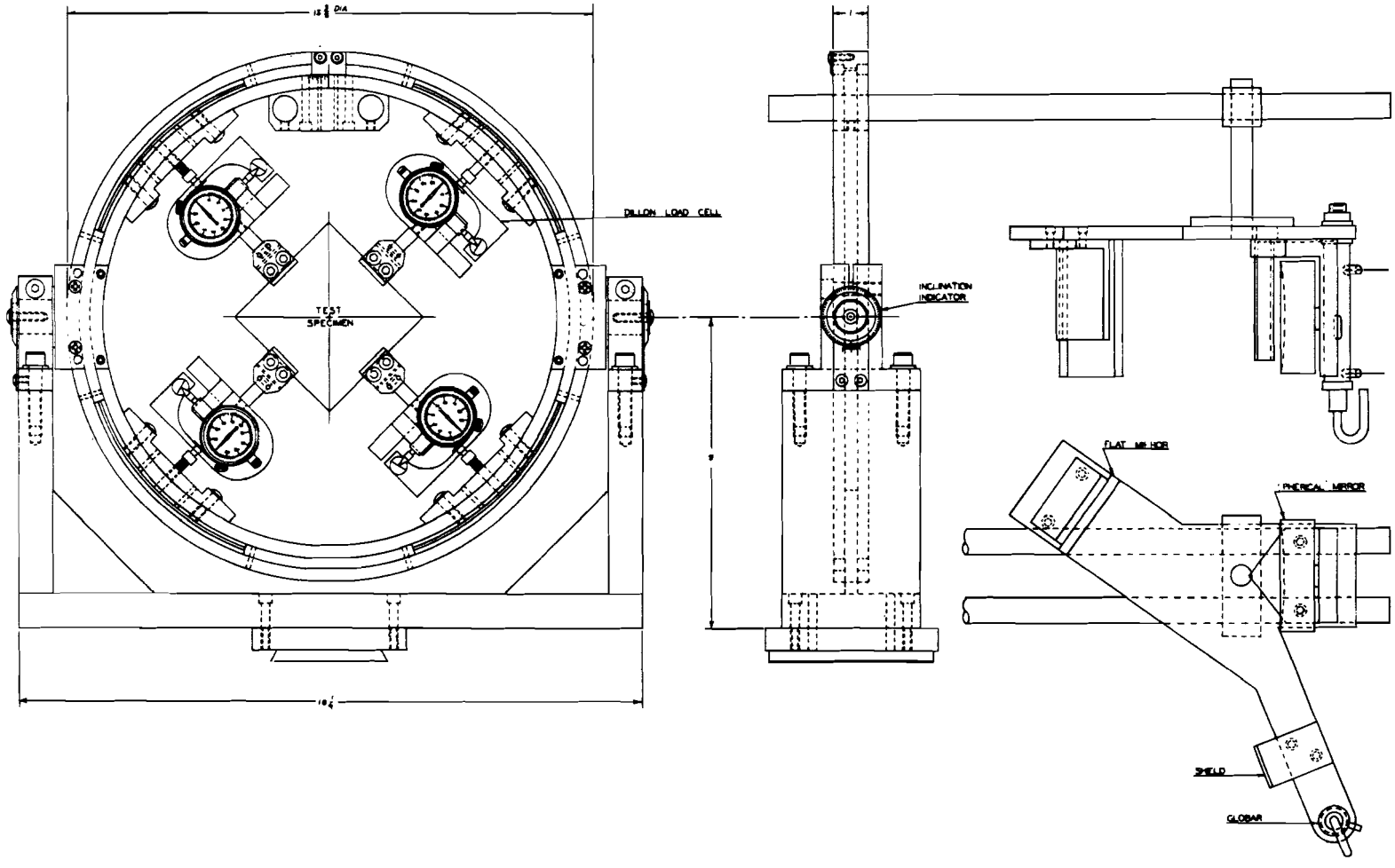

Figure 9 LOADING AND ORIENTATION FIXTURE

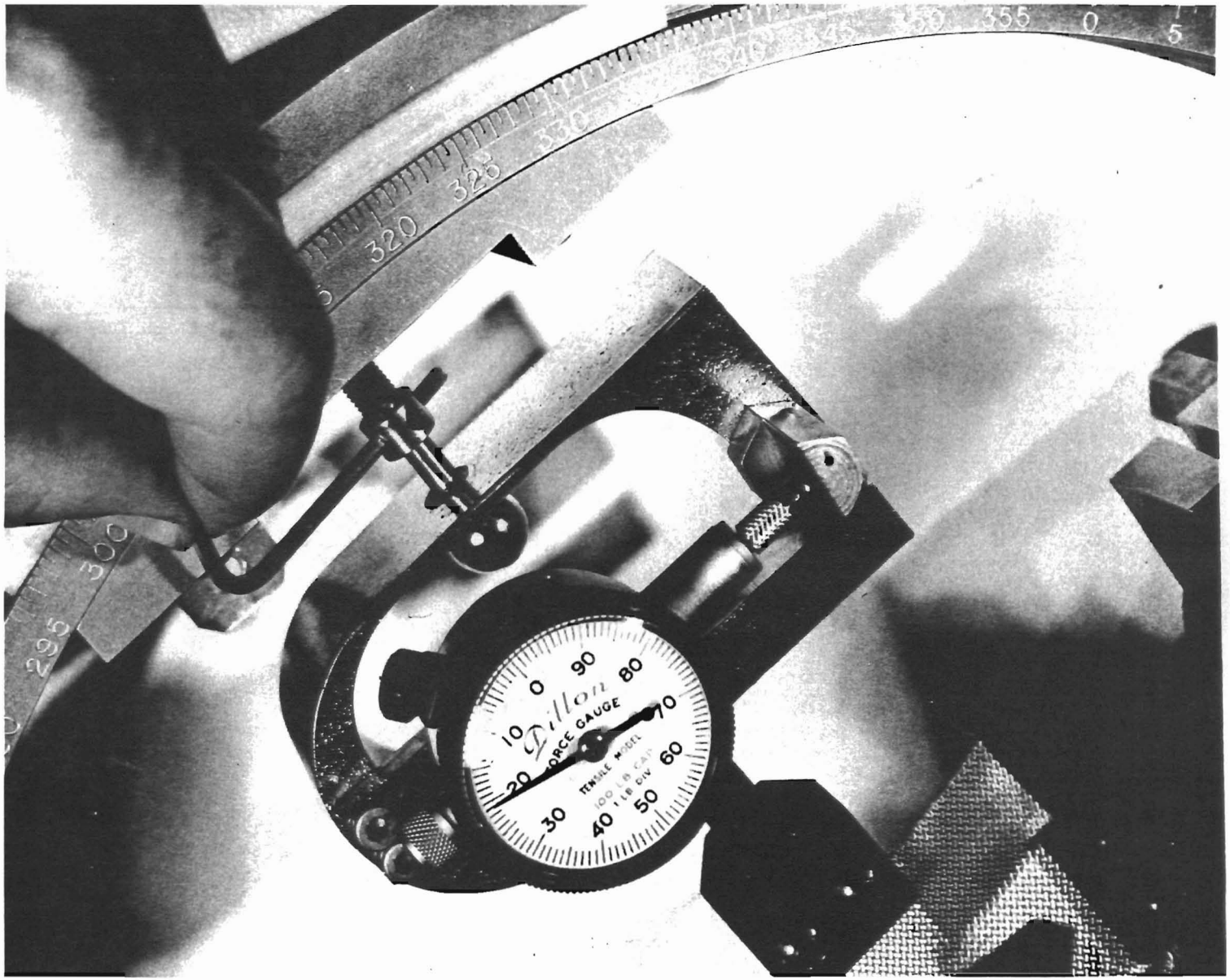

Figure 10 METHOD OF ADJUSTING TENSILE LOAD

A spherical mirror projects an image of the Globar onto the sample (see Figure 11). The image is observed by a second spherical mirror which focuses the radiation into the monochromator entrance slits. The 5 mm diameter Globar is projected onto the sample as a 3 mm width image (see Figure 12). The area of the sample observed by the second spherical mirror was 4.25 mm. This width was considered sufficient to include all of the energy from the multiple scattering effects expected in the woven materials.

The spherical mirror projecting the Globar onto the material is a 3-inch diameter aluminized front surface spherical mirror of 5-3/4 inches focal length located 9 inches from the sample and 15-1/2 inches from the Globar. The second spherical mirror is a 4-1/2-inch diameter spherical mirror with a front surface aluminized coating and a focal length of 16 inches. The mirror is positioned 48 inches away from the material and 22.75 inches from the monochromator. These dimensions and sizes were selected to match the "f" number of the second spherical mirror (f/3.55) to that of the monochromator (f/3.34) so that the energy introduced into the monochromator would not overly exceed the monochromator's maximum viewing angle and thus add to the dispersion within the monochromator.

In order to reduce the energy losses throughout the system, the optical system has been constructed with the use of front surfaced mirrors throughout.

The distance between the sample and detector are held fixed for the measurement of incident as well as reflected and transmitted energies. The same optical components are used for all measurements. Therefore, there is no necessity to calibrate the detection system since only relative magnitudes of energy are needed.

Within the range of wavelengths measured, there is a large variation in the energy levels reaching the detector. At the lower wavelengths (2 to 6 microns) the energy levels are large enough to exceed the peak calibration signal of the amplifier-recorder system. Through communications with the Perkin-Elmer Corporation, it was learned that "the amplifier would become saturated at much lower signals than the thermocouple detector". Upon checking the linearity of the amplifier, it was found that the amplifier was linear up to a 10-microvolt input signal. The largest calibration voltage of the amplifier-record system was 10 microvolts. This meant that the energy reaching the detector must always develop a signal of less than 10 microvolts.

To limit the maximum level of energy reaching the monochromator slits, a wire screen was placed in the optical path between the sample and the monochromator. The screen uniformly decreased the intensity of the energy beam. It was found that the best location for the screen was just in front of the monocrhomator slits (see Figure 13). During the tests, the wire screen is inserted in the beam for the incident energy measurements as well as the reflected and transmitted energy measurements. With a change in wavelength, the screen's position and percentage open area are changed. The screen is placed in the system for all wavelengths up to 6 microns.

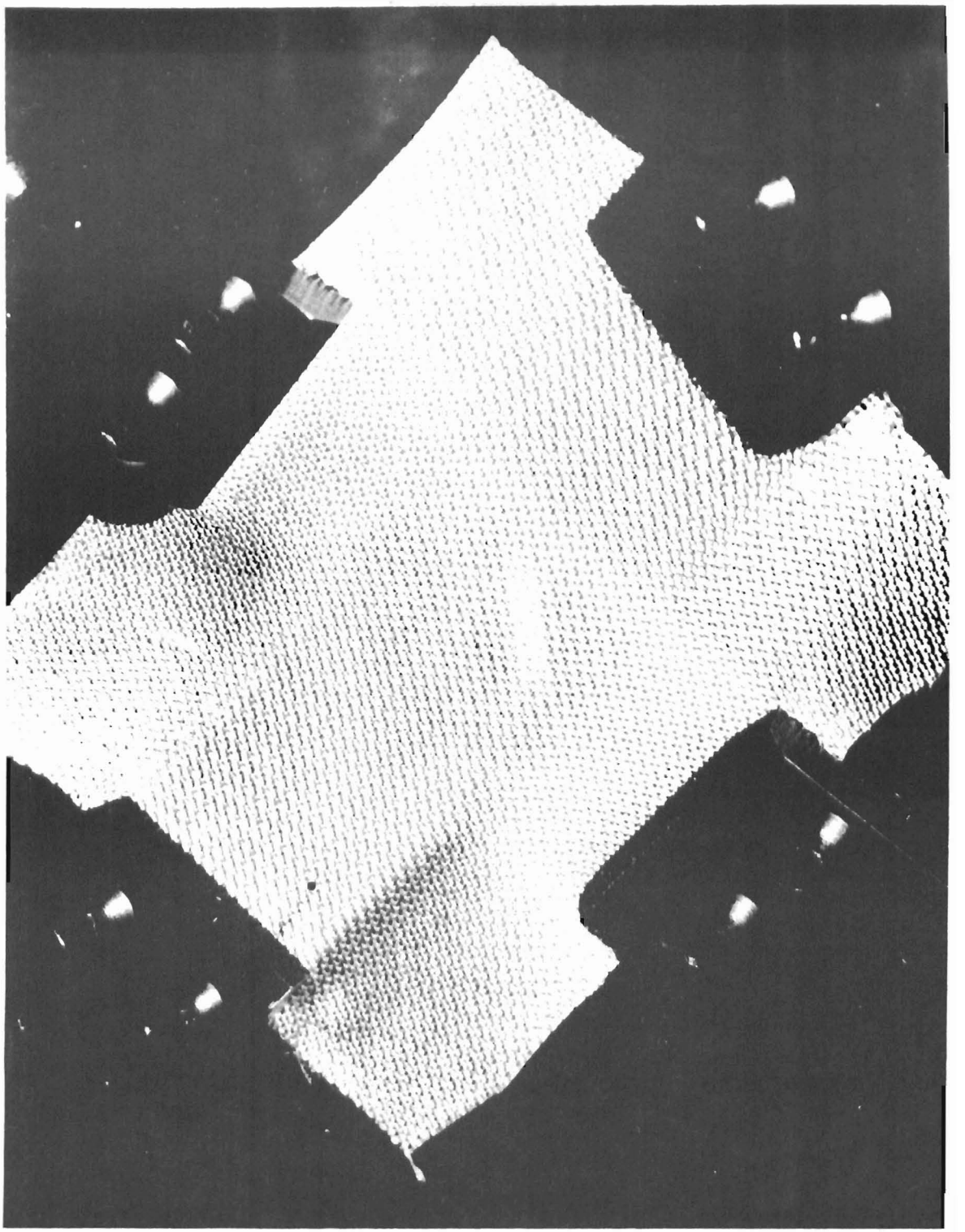

Figure 11 GLOBAR IMAGE ON SAMPLE

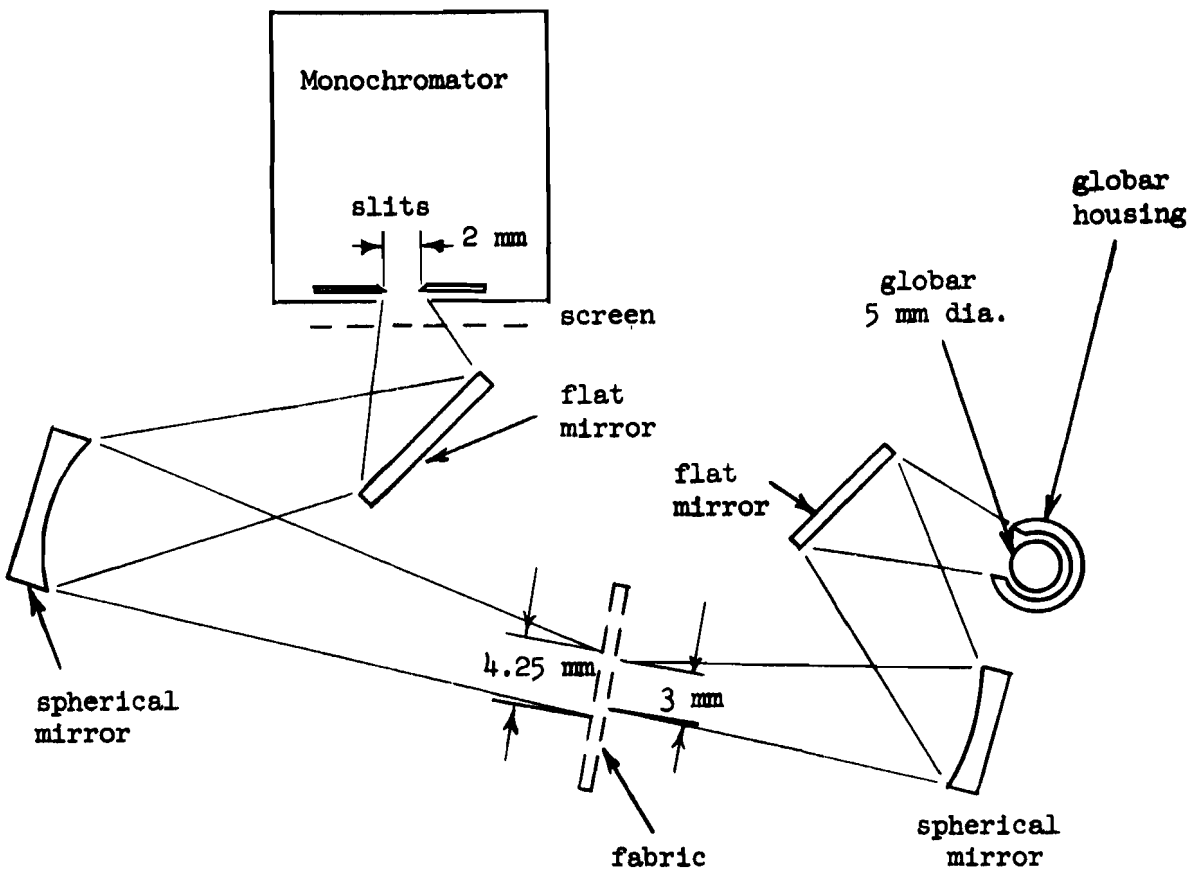

Figure 12 OPTICAL SYSTEM ARRANGEMENT

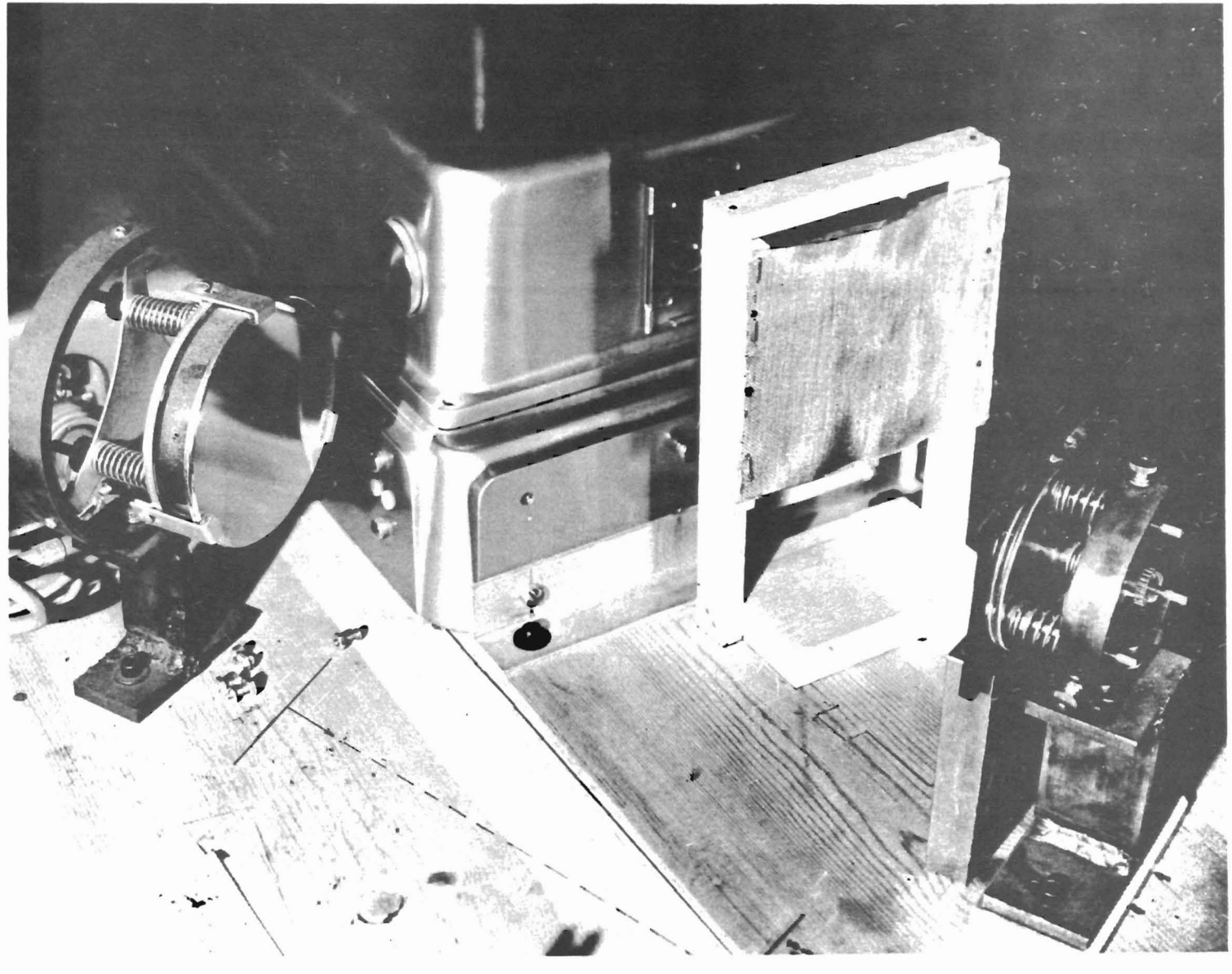

Figure 13 SCREEN IN POSITION

The Globar requires a stabilization time of several hours before it reaches equilibrium. To verify that equilibrium has been achieved and maintained, the voltage and current to the Globar are continuously monitored.

To control the background radiation level, the apparatus has been set in a closed room in which no other high temperature radiative energy sources exist. At this location, the only radiation in the room must come from the walls, floor, and ceiling of the room. Since the room is at a relatively low temperature with respect to the Globar the background energy contribution can be eliminated.

Although the optical system has been rigidly constructed, frequent movement of the loading fixture gradually misaligns the illuminating optical system with respect to the detector optical system. In order to check the alignment of the system a miniature light bulb is placed at the exit slits of the monochromator. The bulb is placed so as to direct light back through the optical system to the material sample. By this procedure, an image of the monochromator entrance slits is projected onto the sample. The green region of the bulb's visible spectrum is selected in order to develop a sharply defined image on the sample. With the Globar turned on, the optical system is adjusted until the image from the Globar is centered within the image of the monochromator slits. This adjustment is complicated by the fact that the two images must remain stationary with respect to each other while the loading fixture is being rotated through the ψ angle (discussed in the next section).

A block diagram illustrating the mechanical, optical, and electrical components of the system is shown in Figure 14. The complete experimental apparatus is shown in Figure 15.

Experimental Procedure

A systematic procedure has been developed for measuring all of the energy emanating from the material. The material as mounted in the fixture can be rotated about two perpendicular axes. One axis is horizontal and the other is vertical. Any angle in space can be defined in terms of the inclination angle, ϕ, and the rotational angle, ψ, (see Figure 16). To obtain a data run, the inclination angle, ϕ, is fixed and the rotational angle, ψ, is scanned 180°. The rotational angle is indexed so that during the 180° rotation, only one side of the material is scanned. At the end of the rotation, the inclination angle is stepped to a new value and the material is scanned again. By continually repeating this process the hemisphere on either side of the material can be surveyed.

Because of the large amount of time (15 minutes) required to manually scan the material about 180° of the ψ axis, the rotational scan was automated (see Figure 17). This was accomplished by driving the loading fixture through the rotational angle, ψ, at a constant angular velocity so that as the ψ angle varied, the detected signal was simultaneously plotted on the recorder. At the end of a scan, the strip-chart record contained a plot of signal intensity versus rotational angle for a fixed ϕ angle and wavelength.

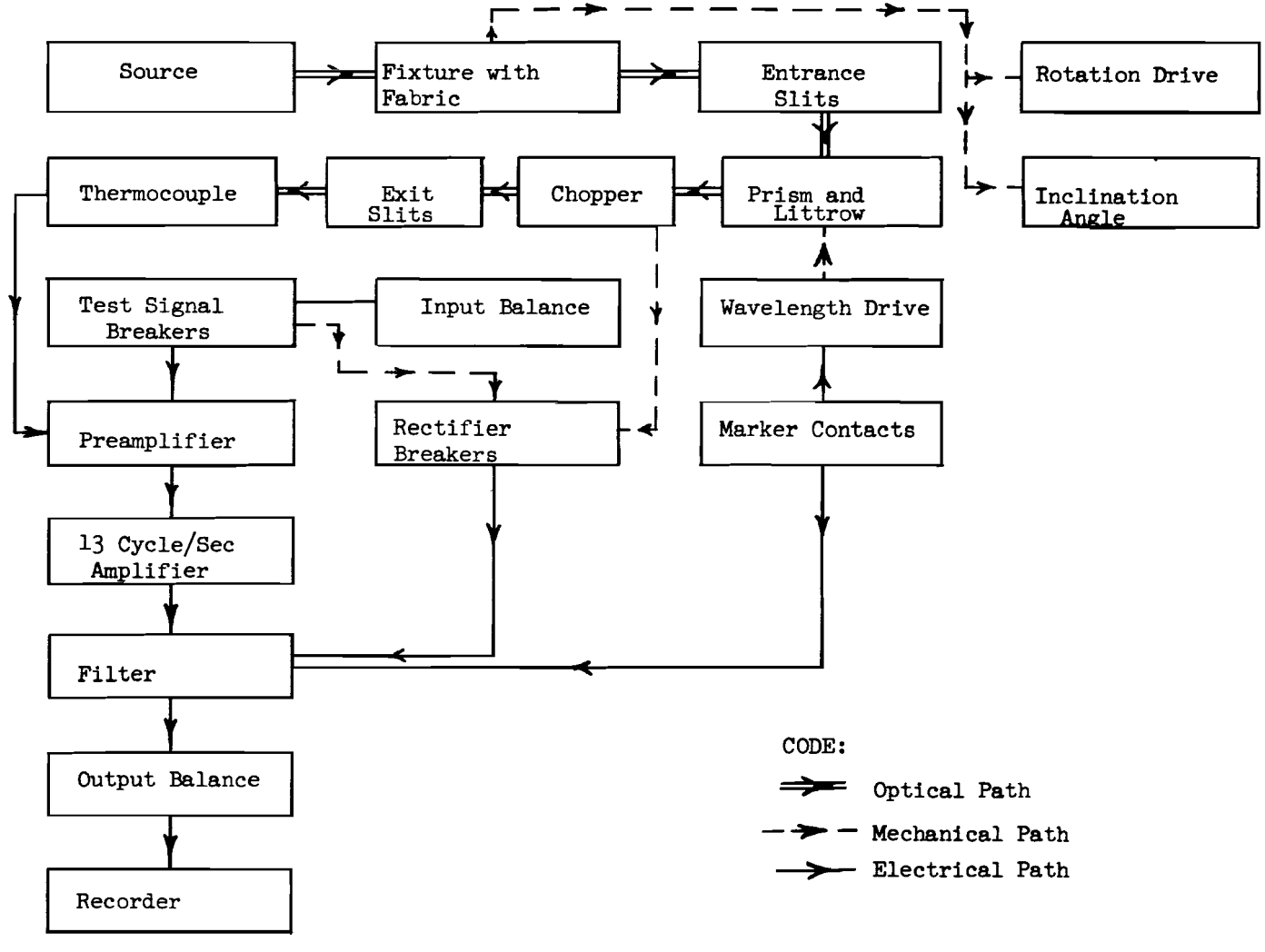

Figure 14 BLOCK DIAGRAM OF EMITTANCE APPARATUS

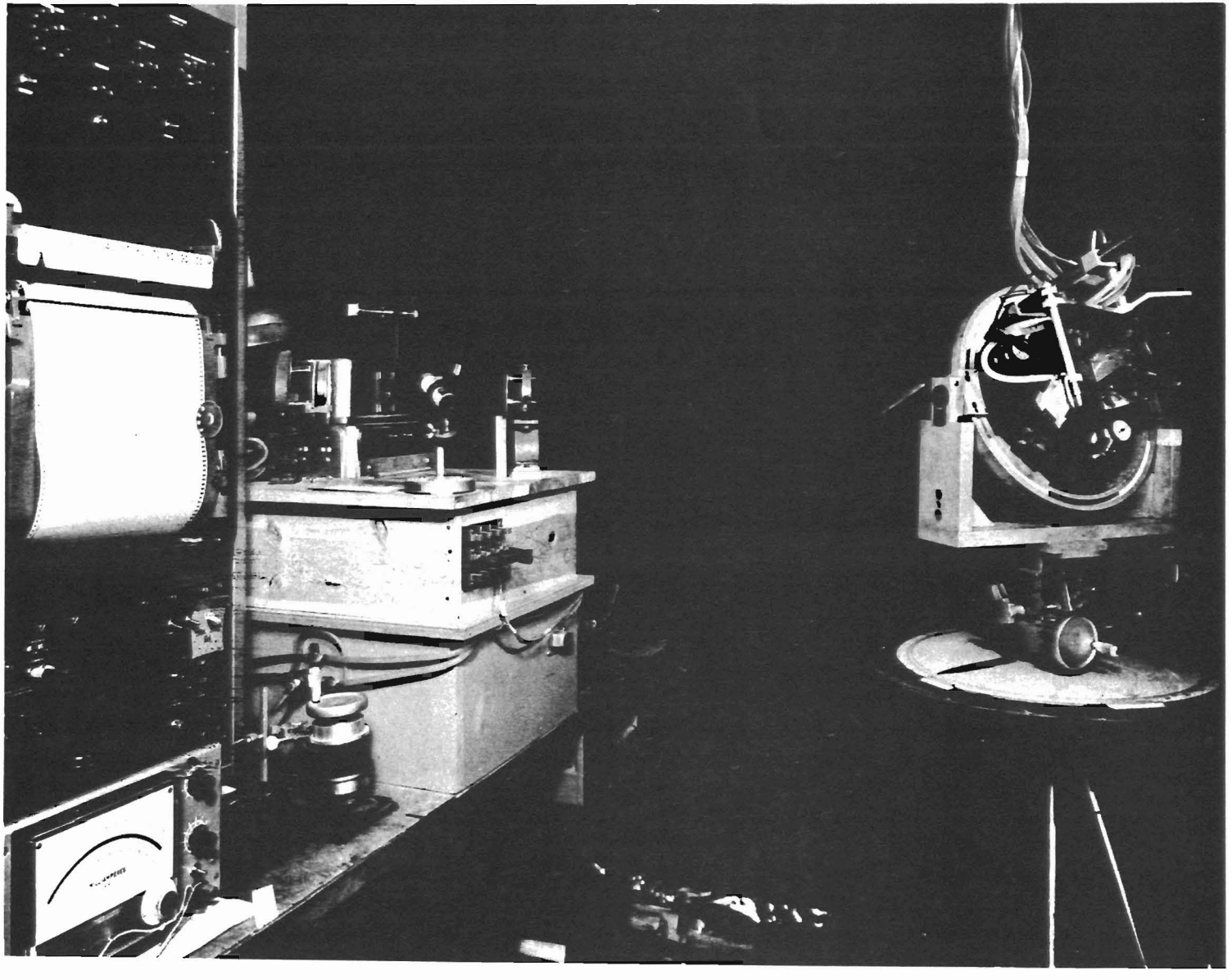

Figure 15 OVERALL VIEW OF EMITTANCE APPARATUS

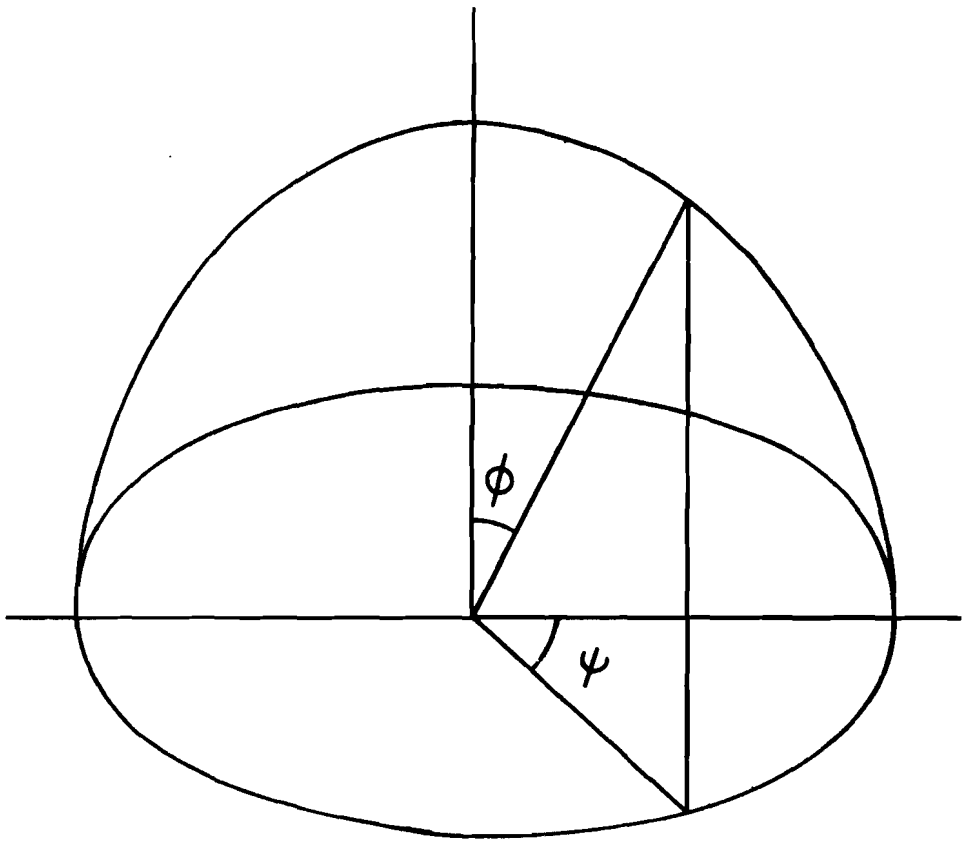

Figure 16 SCANNING ANGLES OF THE DETECTOR RELATIVE TO THE SURFACE OF THE MATERIAL

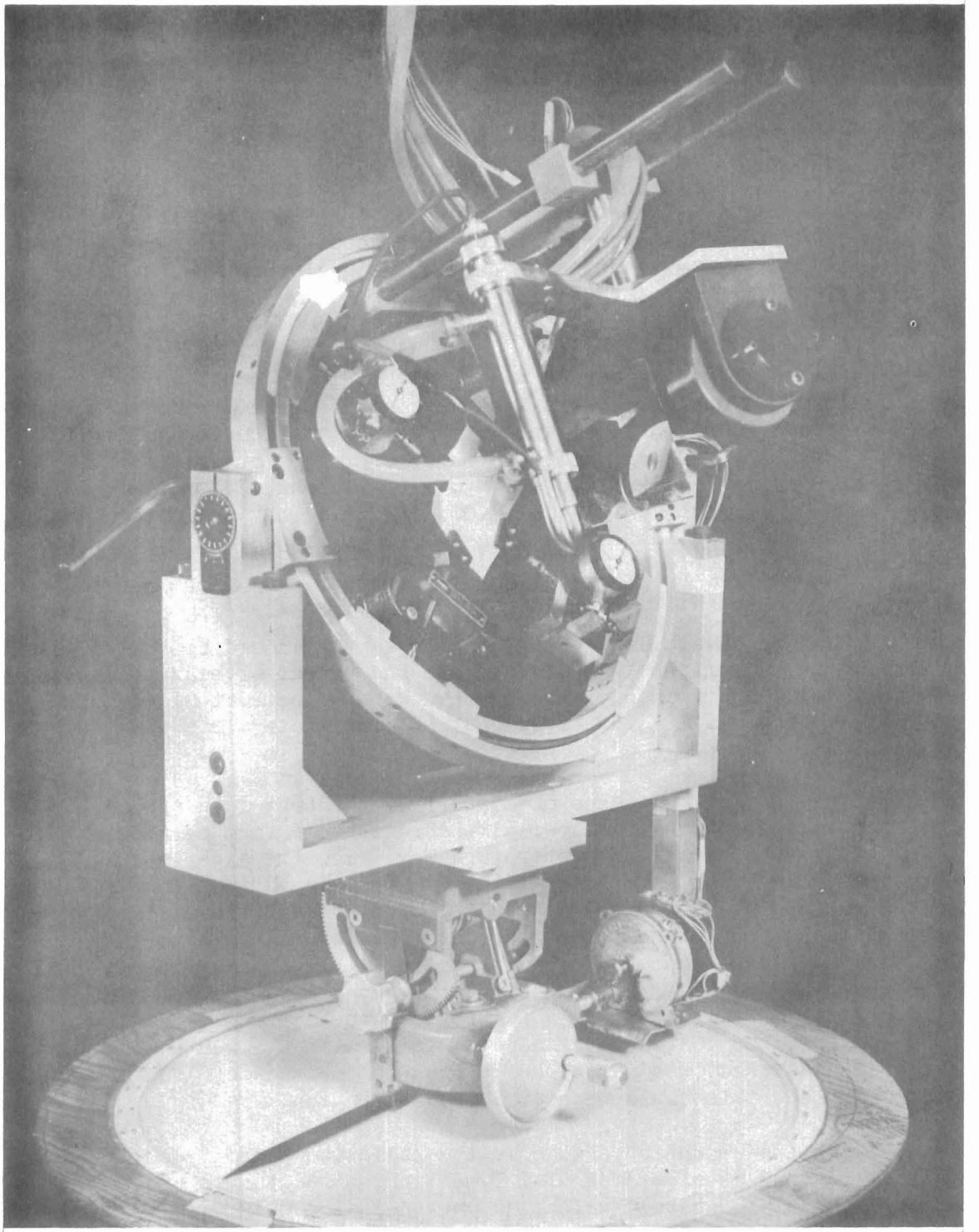

Figure 17 LOADING AND ORIENTATION FIXTURE WITH ψ ANGLE ROTATION MECHANISM

To further increase the speed at which data could be taken, the wavelength setting was accomplished remotedly through the use of two synchro motors and an optical system which permitted remote viewing of the drum turn setting (see Figure 18).

With the present apparatus, one transmittance and one reflectance hemisphere can be scanned every 68 minutes. The time required to canvas the wavelength range of 2 to 15 microns is 16 hours or 2 work days. In practice no data were collected beyond 9 microns. This is due to the fact that at wavelengths greater than 7 microns the trace on the strip records has a high noise level associated with it. The extraction of the true signal from the "hash" is extremely difficult, if not impossible, to accomplish. As a result, data beyond 7 microns was difficult to obtain.

The spectral absorptance curves all show absorption bands at 2 microns, 5 microns, and 7 to 9 microns. This study was not concerned with the nature of these causative agents and thus no attempt was made to identify them. In Reference 8, Dunkle, Ehrenburg, and Gier have reported similar absorption bands in organic materials at 3-3.5 microns, 5.75-6.00 microns, 7.25 microns, 7.75 microns, 7.00-9.00 microns, and 14.00-17.00 microns. They indicated that certain alkanes, alkenes, alkynes, esters, and the carbon-hydrogen bond are probably the causative molecular group.

The data were derived while the samples were under a state of biaxial tension. With the time and funds available, each of the samples could be tested under only one value of biaxial tension. To investigate the effect of biaxial tension upon the resultant data, a specimen of HT-1 Type I was subjected to loads of 15, 30, 45, and 60 ppi. The results indicated that spectral data are a weak friction of biaxial tension.

The spectral normal emittance obtained from the test data are applicable up to the temperature at which the material undergoes some form of physical alteration. To establish the maximum temperature for which the experimental results could be applicable, samples of each material were placed in a furnace. The furnace temperature was increased by 100°F increments and the materials were inspected at each temperature. The materials were examined as to their color, rigidity, and tear resistance at each inspection. All of the materials remained unchanged up to 400°F. Beyond this point, the changes introduced were a function of the material. In all cases where a material was heated with a coating and without a coating, the coated material deteriorated at a lower temperature. The furnace, which was used, was capable of a peak temperature of 1800°F. As a result, not all of the materials could be heated to destruction.

To evaluate the amount of change in the radiation properties induced by the physcial alterations, a sample of HT-1 Type I which had turned brown at 700°F and a sample of Renē 41 (uncoated) which had darkened at 1400°F were tested. The HT-1 Type I did not appreciably change its transmittance and reflectance spectral values when it became colored. The Renē 41, after heating, produced a spectral

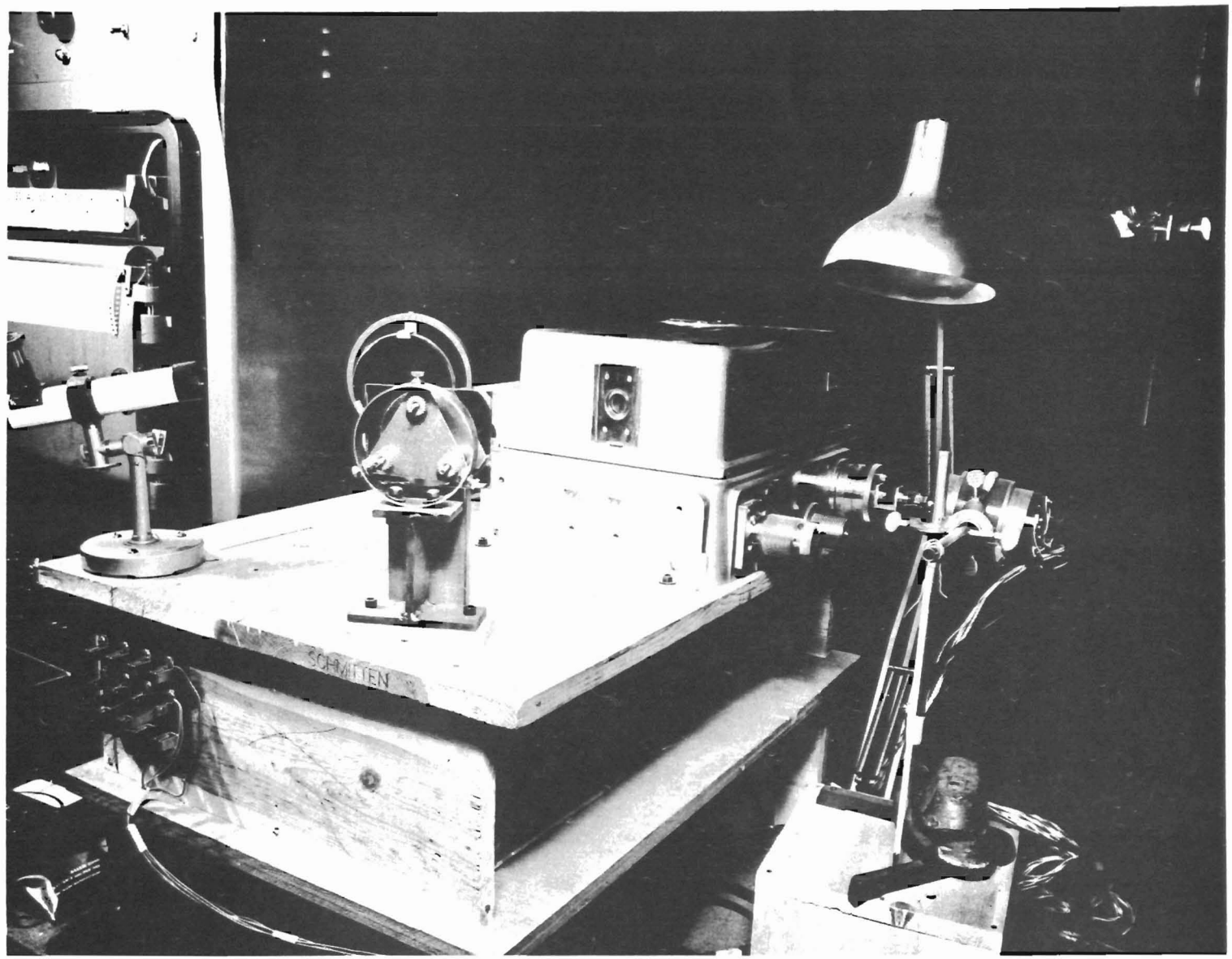

Figure 18 REMOTE WAVELENGTH CHANGE MECHANISM

transmittance curve which was similar to that developed when the material was in its "as received" state but its spectral reflectance values had changed considerably. These results indicate that altered fabric appearances may not necessarily change the infrared radiation properties of the material. Due to a shortage of time and funds, this study could not be more fully investigated.

The observed data permits direct computation of spectral normal emittance values. Values of total hemispherical emittance are required to estimate the heat loss or gain from the material surfaces. Equation (25) is used to compute the values of total normal emittance in the form

$$\epsilon_{normal} = \frac{\int_{\lambda_{min}}^{\lambda_{max}} \epsilon_{\lambda,\,normal} \frac{d\dot{Q}_{bb}}{d\lambda} d\lambda}{\int_{\lambda_{min}}^{\lambda_{max}} \frac{d\dot{Q}_{bb}}{d\lambda} d\lambda} \tag{33}$$

where: λ_{max} = maximum wavelength for which there is spectral data

λ_{min} = minimum wavelength for which there is spectral data

The description of the emittance value ϵ_{normal} as the total normal emittance value is misleading since the value of ϵ_{normal} does not include the spectral range less than λ_{min} or greater than λ_{max}. The computed total normal emittance value (based upon the wavelength interval of $\lambda_{min} \leq \lambda \leq \lambda_{max}$) can be considered a valid result if a major portion of the energy emitted by the material at a temperature resides in the wavelength interval. The larger the percentage of energy, the greater the validity of the computed total normal emittance value.

In a similar manner, the total normal reflectance and transmittance can be computed respectively by

$$\rho_{normal} = \frac{\int_{\lambda_{min}}^{\lambda_{max}} \rho_{\lambda,normal} \frac{d\dot{Q}_{bb}}{d\lambda} d\lambda}{\int_{\lambda_{min}}^{\lambda_{max}} \frac{d\dot{Q}_{bb}}{d\lambda} d\lambda} \tag{34}$$

and

$$\tau_{normal} = \frac{\int_{\lambda_{min}}^{\lambda_{max}} \tau_{\lambda,normal} \frac{d\dot{Q}_{bb}}{d\lambda} d\lambda}{\int_{\lambda_{min}}^{\lambda_{max}} \frac{d\dot{Q}_{bb}}{d\lambda} d\lambda} \tag{35}$$

The emittance values determined are total normal emittance. To establish the heat transfer rates for a material, values of total hemispherical emittance must be available. The total hemispherical emittance can be obtained from the total normal emittance by utilizing the information presented by Jacob (Reference 4) for the ratio of these values for conducting and nonconducting materials. Jacob shows that the ratio of total hemispherical emittance to total normal emittance is 1.33 to 1.05 for electrically conducting materials and 1.05 to 0.95 for electrically nonconducting materials.

Experimental Reproducibility and Error

Data are obtained from the thermal emittance apparatus in the form of strip-chart records. Through experience it has been found that a trace on the strip-chart can be reproduced to within $\pm$ 4%. The integration of the traces and the integration of these results is reproducible to within $\pm$ 1%. If both of these deviations were maximized the resultant spectral data would be reproducible to within $\pm$ 5%. All of the spectral data for transmitted, reflected, and incident energies are reproducible to within $\pm$ 5%. With these data the resultant spectral emittance values are reproducible to within $\pm$ 7%.

The absolute accuracy of the emittance data can be established through the use of emittance standards or analytical predictions. To date, there are no known standards for emittance determinations made at room temperature. Also, there are no analytical prediction procedures available for woven materials.

One material which is used as a secondary standard is magnesium oxide. It is used in the form of a coating that has been smoked onto a metal plate. Magnesium oxide must be tested as a freshly prepared sample since its reflectance changes as the coating ages (See Reference 9).

Almost all of the literature that has been published of magnesium oxide spectral reflectance do not describe the thickness of the oxide coating or the nature and physical surface preparation of the base metal. Without this information, the reflectance values cannot be reproduced without error.

Spectral reflectance data were obtainable only from 2 to 5 microns due to the low level of the detector signal above 5 microns. These data were compared to the results of Gier, Dunkle, and Bevens (see Reference 10). The values at 2 and 3 microns agreed to within 3%. The values a 4 and 5 microns differed greatly but this is in the spectral region where the base metal surface effects the results. The large discrepancy between the values cannot be completely explained by the base metal effect since the reflectance of a black painted surface is on the order of 0.7 for the 4 and 5 micron range. As a result, the magnesium oxide tests were considered inconclusive.

Uncertainty in the exact preparation of the magnesium oxide sample lead to a quest for samples that have been tested in other facilities. Two such samples were obtained from Dr. D. K. Edwards of the UCLA Radiation Laboratory. One sample was a slab of fused silica and the other an aluminum disk painted with an aluminum paint in a silicon-alkyd vehicle.

The fused silica results compared rather closely. The aluminum disk data were seen to be a fairly consistent 25% less than the values obtained by UCLA. This disagreement is understandable since the experimental data show the aluminum disk to be reflecting most of its energy in a specular manner. This is the type of sample which the emittance apparatus is least capable of handling, therefore a lower valued spectral reflectance curve is to be expected.

To obtain a better comparison of these sets of data, total normal emittance values were computed for each of the four sets of data. The results indicate that the total normal emittances found by the MRD emittance apparatus agree to within 29% of the UCLA data. If the latter data are considered to be the correct values, this would imply that the measured emittances can be subject to errors as large as 30%. In actuality, the UCLA data are not absolutely correct since they can contain errors in the reflectance values of $\pm$ 0.03 (Reference 8).

A series of tests were run to determine the sensitivity of the data to specimen positioning errors. A magnesium oxide sample was positioned at various locations near the fabric holding fixture and the reflectances measured at 2, 3, 4 and 5 microns. The curves show that the resulting reflectances reach their maximum values over a distance of about 3/16 inch. The apparatus could maintain the surfaces in a fixed position with a variation of $\pm$ 1/16 inch. This variation in position could introduce a variation in the data and is likely a contributing factor to the total data reproducibility of $\pm$ 5%.

In the data reduction, the energy emitted by the material was considered negligible. This assumption is justified by the curves of Figure 19. The energy incident upon the material is emitted by the Globar at 2200°F. This energy is partially absorbed by the material raising its temperature and causing it to emit energy. With the room temperature at 75°F, the material has been found to be emitting at a maximum of 100°F. Figure 19 shows that the resultant energy from the material is less than 0.1% of the energy emitted by the Globar. Thus, the energy emitted by the material can be considered negligible with at most a 0.1% possible error in the emittance value.

Localized Temperature Measurement Validity Check

A device was constructed to evaluate local material temperatures. It is shown in Figure 20. In the apparatus a jet of heated air was directed against a fabric sample held vertically in a fixture. By means of this air jet it was possible to heat the material to any temperature up to 1500°F. The temperature of the material was sensed by a thermocouple woven into the material (see Figure 21). A chromel-constantan HT* micro-miniature thermocouple of 0.014-inch diameter with a 90% platinum and 10% rhodium sheath was used.

* Tradename of Baldwin-Lima-Hamilton Co.

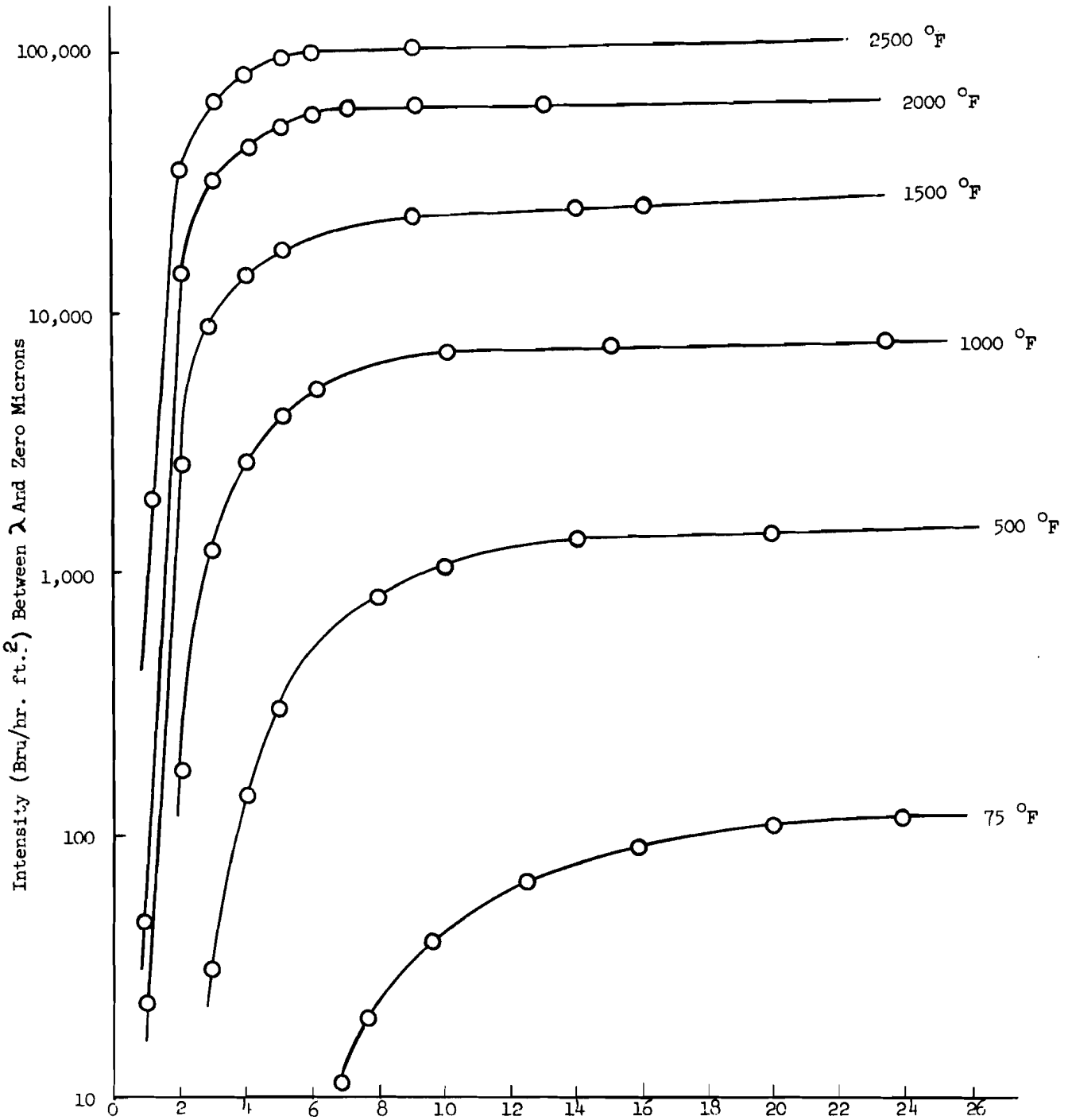

Figure 19 BLACKBODY INTENSITY DISTRIBUTIONS AS A FUNCTION OF WAVELENGTH DIFFERENCES AND TEMPERATURE

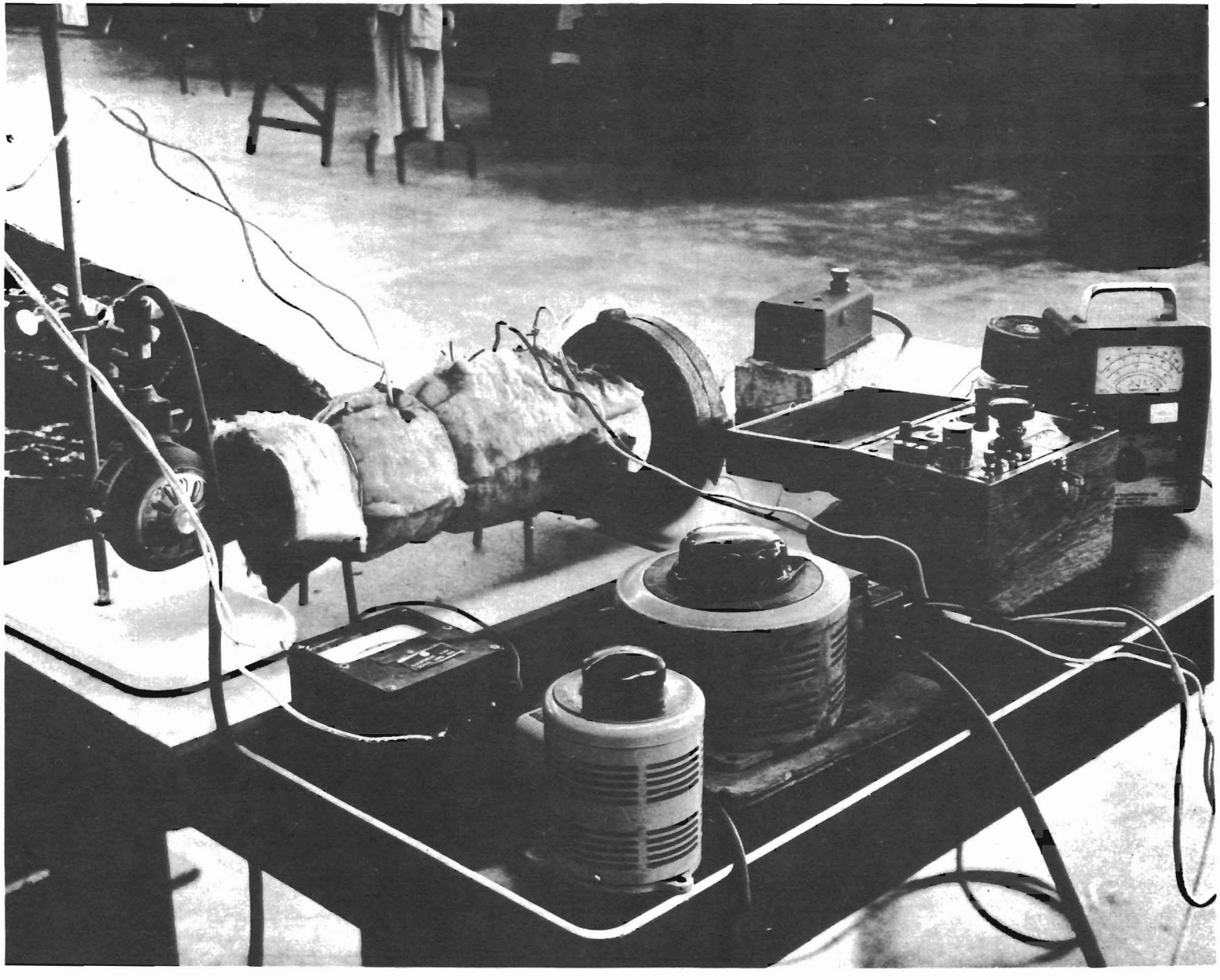

Figure 20 OVERALL VIEW OF TRANSDUCER EVALUATION APPARATUS

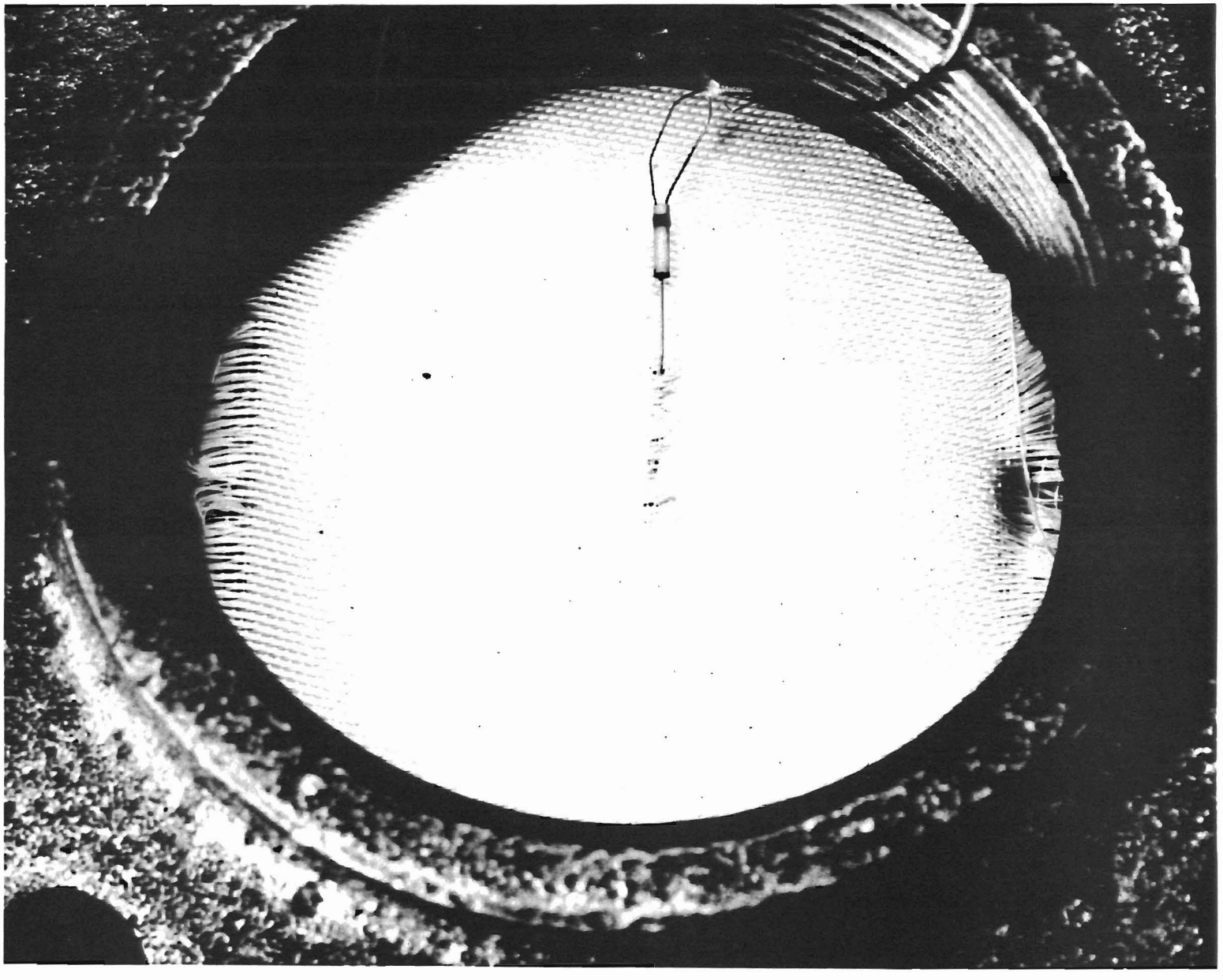

Figure 21 TRANSDUCER WOVEN INTO MATERIAL SAMPLE OF VITREOUS SILICA (UNCOATED)

The effect of thermocouple position was investigated to determine the maximum temperature variation that could be measured in and around the material. It was found that maximum variations of 60°F could be measured at a 600°F temperature level. This variation was obtained with the thermocouple in various positions from the front to the back of the material. By controlling the placement of the thermocouple so that the bead would always remain buried in a strand of the material, a 30°F variation was found through the material. This amounted to a 5% variance at the 600°F temperature level. By changing the temperature level, the temperature variance was found to be from 5 to 10% of the temperature level. This result was not a function of the material tested. The tested materials were limited to those which had multi-filament strands in which the thermocouple could be embedded.

The heated fabrics were viewed by a total radiation pyrometer* focused on a 0.1-inch diameter area of the material. The emittance value deduced from the spectral emittance apparatus was set into the pyrometer. Comparing the pyrometer determined temperature to that given by the thermocouple it is possible to obtain an indication of the accuracy of the thermocouple reading. The pyrometer was focused at various points within a 1/8-inch diameter area centered about the head of the embedded thermocouple. Within this area, temperature variations of as much as 100°F were indicated. It was previously stated that the placement of the thermocouple would vary the temperature reading by as much as 10%. This would account for the temperature descripancies which exist between the pyrometer and the thermocouple.

The thermocouple is seen to measure temperatures which vary by 10% of each other. Since this identical result has been obtained with the pyrometer and because the detectors operate on two entirely different principles, the true localized temperatures of the material are considered detectable to within 10%.

* Thermodat Pyrometer Model TD6BT-15 made by the Radiation Electronics Company Division of the Comptometer Corporation.

CONCLUSIONS

Thermal Conductance

A transient, calorimetric technique was developed capable of measuring the thermal conductance of thin, flexible materials. The apparatus permits control of environmental parameters of temperature, ambient pressure, biaxial tension and compression over the following ranges.

Temperature,	200 to 1500°F
Ambient Pressure,	0.4 mm Hga to 20.2 psia
Biaxial Tension,	1.0 to 109 ppi
Compression,	1.9 to 13.7 psi

Calibration and verification tests of the apparatus agreed to within 7% of the thermal conductance of Asbestos paper and Mylar film at low temperature (approximately 200°F). A reliable calibration standard over a range of temperatures and in particular at high temperature (approaching 1500°F) could not be found.

Fourteen candidate fibrous structural materials were supplied by and/or acquired for the Air Force and were tested to determine their thermal conductance and thermal emittance. The thermal conductance measurements were found to exhibit an average reproducibility of 8.7% for which data obtained were linear to an average of 0.5%.

With the extensive amount of data collected during the present program it is evident that thermal conductance is influenced by the environmental conditions imposed. The thermal conductance of the fibrous structural materials at reduced (vacuum) pressures are lower by a factor of two than those at ambient pressures. In addition, generally the conductance tended to increase in value with increasing temperature.

Several comparative relationships were established by the test program. It was found that the thermal conductances and diffusivities of two nylons were equal at the two pressure levels although the weaves of the materials differed. The conductances and diffusivities for the HT-1 Types I and II followed a similar trend. The HT-1 Type III however, had values which were a factor of two greater than those for Types I and II. The HT-1 Type III is a material which has much less void space in its weave than the other types.

Noting that the thermal conductance is a compound property, defined as a combination of convective, radiative and conductive modes of transfer, the fact that reducing the porosity per unit volume of material (as demonstrated by HT-1 Type III compared to HT-1 Types I and II) produced greater conductance values indicates that the conductive mode of heat transfer predominates over the radiative and convective modes.

In comparing the results for the coated and uncoated materials, the absence or presence of a coating was found to have no effect upon the thermal conductance of the material. This can be explained by the fact that the conductance value is dependent upon the properties of the bulk material of the fabric and the coatings added little mass to the main constituent of the fabric. The small mass addition of the coating could not appreciably alter the average properties of the coating and constituent combination. On the other hand, in determining the compressive stress-strain relationships for the materials, the coated materials were found to consistently develop lower values of strain for a given value of stress when compared to the uncoated materials. This indicated the coatings had caused the uncoated material to become more ductile.

The thermal conductances measured varied from a high of 0.14 Btu/hr ft°F for graphite cloth to a low of 0.02 Btu/hr ft°F for Nylon and the HT-1 fabrics. The thermal diffusivities computed ranged from 0.013 to 0.001 ft^2/hr. Thus, both thermal conductance and diffusivity for the materials investigated ranged within one order of magnitude.

Thermal Emittance

The results have proved that the developed technique is capable of measuring the spectral emittance of thin, semi-transparent specimens. The data obtained have a reproducibility of $\pm$ 7%.

Tests indicated that the spectral reflectivity and transmissivity were a weak function of changes in biaxial tension over the range of 15 to 60 ppi for the HT-1 Type I fabric. As a result, it is anticipated that the spectral characteristic of the materials are weak functions of temperature.

The data obtained for the HT-1 Type I and uncoated René 41 materials indicate that the infrared data, derived at room temperature, can be used in the determination of higher temperature emittance values. This extrapolation is permissible until the temperature is reached where the physical characteristics of the material change. Thus, the spectral data that have been obtained permit the computation of total emittance over a range of material temperatures.

In comparing the temperatures at which physical characteristics of the materials changed, it was found that all of the coated materials were physically altered at lower temperatures than the respective uncoated materials. But the total normal emittance values for the coated materials were from 10 to 30%

greater than those for the uncoated materials. Thus it is possible that with their greater capability to radiate larger quantities of heat the coated materials can remain at lower equilibrium temperatures than the uncoated materials.

In general there was no single material that had a predominantly high total normal emittance value. Most of the materials had total normal emittance values in the range of 0.45 to 0.65.

A summary of the data obtained for the thermal transport and radiative properties is presented in Tables 1 and 2.

TABLE 1

SUMMARY OF THERMAL PROPERTIES OF FIBROUS STRUCTURAL MATERIALS

1N Nylon (0.0146 lb/ft^2)

	Temperature (°F)	Avg. Therm. Conductance (Btu/hr ft °F)	Specific Heat (Btu/lb°F)	Thickness Under Load (ft)	Density (lb/ft^3)	Thermal Diffusivity (ft^2/hr)
Ambient Pressure	100	0.027	0.40	0.00038	38.2	0.0018
	200	0.025	0.48	0.00038	38.2	0.0014
	300	0.024	0.53	0.00038	38.2	0.0012
	400	0.022	0.57	0.00038	38.2	0.0010
Vacuum	100	0.008	0.40	0.00038	38.2	0.00052
	200	0.010	0.48	0.00038	38.2	0.00055
	300	0.013	0.53	0.00038	38.2	0.00064
	400	0.015	0.57	0.00038	38.2	0.00069

11N Nylon (0.0143 /ft^2)

	Temperature (°F)	Avg. Therm. Conductance (Btu/hr ft °F)	Specific Heat (Btu/lb°F)	Thickness Under Load (ft)	Density (lb/ft^3)	Thermal Diffusivity (ft^2/hr)
Ambient Pressure	100	0.023	0.40	0.000476	30.1	0.0019
	200	0.022	0.48	0.000476	30.1	0.0015
	300	0.022	0.53	0.000476	30.1	0.0014
	400	0.021	0.57	0.000476	30.1	0.0012
Vacuum	100	0.008	0.40	0.000476	30.1	0.00066
	200	0.009	0.48	0.000476	30.1	0.00062
	300	0.010	0.53	0.000476	30.1	0.00063
	400	0.013	0.57	0.000476	30.1	0.00076

Pluton Cloth (0.0555 lb/ft^2)

	Temperature (°F)	Avg. Therm. Conductance (Btu/hr ft °F)	Specific Heat (Btu/lb°F)	Thickness Under Load (ft)	Density (lb/ft^3)	Thermal Diffusivity (ft^2/hr)
Ambient Pressure	200	0.024	*	0.000891	62.3	*
	400	0.026	*	0.000891	62.3	*
	600	0.031	*	0.000891	62.3	*
	800	0.040	*	0.000891	62.3	*
Vacuum	200	0.008	*	0.000895	62.0	*
	400	0.011	*	0.000895	62.0	*
	600	0.014	*	0.000895	62.0	*
	800	0.020	*	0.000895	62.0	*

HT1-Type I (0.0135 lb/ft^2)

	Temperature (°F)	Avg. Therm. Conductance (Btu/hr ft °F)	Specific Heat (Btu/lb°F)	Thickness Under Load (ft)	Density (lb/ft^3)	Thermal Diffusivity (ft^2/hr)
Ambient Pressure	400	0.021	0.35	0.000479	28.3	0.0038
	500	0.022	0.35	0.000479	28.3	0.0041
	600	0.025	0.35	0.000479	28.3	0.0045
	700	0.028	0.35	0.000479	28.3	0.0051
Vacuum	400	0.008	0.35	0.000479	28.3	0.0014
	500	0.009	0.35	0.000479	28.3	0.0016
	600	0.010	0.35	0.000479	28.3	0.0018
	700	0.012	0.35	0.000479	28.3	0.0022

HT1-Type II (0.0213 lb/ft^2)

	Temperature (°F)	Avg. Therm. Conductance (Btu/hr ft °F)	Specific Heat (Btu/lb°F)	Thickness Under Load (ft)	Density (lb/ft^3)	Thermal Diffusivity (ft^2/hr)
Ambient Pressure	400	0.020	0.35	0.000674	31.6	0.0018
	500	0.022	0.35	0.000674	31.6	0.0020
	600	0.024	0.35	0.000674	31.6	0.0022
	700	0.027	0.35	0.000674	31.6	0.0025
Vacuum	400	0.010	0.35	0.000670	31.8	0.00090
	500	0.012	0.35	0.000670	31.8	0.00110
	600	0.015	0.35	0.000670	31.8	0.00135
	700	0.018	0.35	0.000670	31.8	0.00163

HT1-Type III (0.0430 lb/ft^2)

	Temperature (°F)	Avg. Therm. Conductance (Btu/hr ft °F)	Specific Heat (Btu/lb°F)	Thickness Under Load (ft)	Density (lb/ft^3)	Thermal Diffusivity (ft^2/hr)
Ambient Pressure	400	0.043	0.35	0.00121	35.5	0.0034
	500	0.045	0.35	0.00121	35.5	0.0036
	600	0.049	0.35	0.00121	35.5	0.0039
	700	0.054	0.35	0.00121	35.5	0.0044
Vacuum	400	0.021	0.35	0.00121	35.5	0.0017
	500	0.024	0.35	0.00121	35.5	0.0019
	600	0.027	0.35	0.00121	35.5	0.0022
	700	0.031	0.35	0.00121	35.5	0.0025

FIBERGLASS CLOTH (0.0618 lb/ft^2)

	Temperature (°F)	Avg. Therm. Conductance (Btu/hr ft °F)	Specific Heat (Btu/lb°F)	Thickness Under Load (ft)	Density (lb/ft^3)	Thermal Diffusivity (ft^2/hr)
Ambient Pressure	400	0.038	0.24	0.00110	56.3	0.0028
	600	0.038	0.26	0.00110	56.3	0.0026
	800	0.041	0.27	0.00110	56.3	0.0026
	1000	0.047	0.28	0.00110	56.3	0.0030
	1200	0.057	0.29	0.00110	56.3	0.0035
Vacuum	400	0.024	0.24	0.00107	57.9	0.0017
	600	0.022	0.26	0.00107	57.9	0.0015
	800	0.023	0.27	0.00107	57.9	0.0015
	1000	0.027	0.28	0.00107	57.9	0.0017
	1200	0.035	0.29	0.00107	57.9	0.0021

ALUMINIZED FIBERGLASS

	Temperature (°F)	Avg. Therm. Conductance (Btu/hr ft °F)	Specific Heat (Btu/lb°F)	Thickness Under Load (ft)	Density (lb/ft^3)	Thermal Diffusivity (ft^2/hr)
Ambient Pressure	400	0.038	*	0.000707	*	*
	600	0.036	*	0.000707	*	*
	800	0.036	*	0.000707	*	*
	1000	0.040	*	0.000707	*	*
	1200	0.049	*	0.000707	*	*
Vacuum	400	0.013	*	0.000706	*	*
	600	0.018	*	0.000706	*	*
	800	0.022	*	0.000706	*	*
	1000	0.023	*	0.000706	*	*
	1200	0.021	*	0.000706	*	*

GRAPHITE CLOTH (0.053 lb/ft^2)

	Temperature (°F)	Avg. Therm. Conductance (Btu/hr ft °F)	Specific Heat (Btu/lb°F)	Thickness Under Load (ft)	Density (lb/ft^3)	Thermal Diffusivity (ft^2/hr)
Ambient Pressure	400	0.120	0.40	0.00172	30.9	0.0097
	600	0.136	0.40	0.00172	30.9	0.0110
	800	0.149	0.40	0.00172	30.9	0.0121
	1000	0.159	0.40	0.00172	30.9	0.0128
	1200	0.166	0.40	0.00172	30.9	0.0134
Vacuum	400	0.075	0.40	0.00168	31.6	0.00593
	600	0.082	0.40	0.00168	31.6	0.00649
	800	0.091	0.40	0.00168	31.6	0.00720
	1000	0.103	0.40	0.00168	31.6	0.00815
	1200	0.120	0.40	0.00168	31.6	0.00949

VITREOUS SILICA (UNCOATED) (0.0664 lb/ft^2)

	Temperature (°F)	Avg. Therm. Conductance (Btu/hr ft °F)	Specific Heat (Btu/lb°F)	Thickness Under Load (ft)	Density (lb/ft^3)	Thermal Diffusivity (ft^2/hr)
Ambient Pressure	400	0.047	0.24	0.00129	51.5	0.0038
	600	0.042	0.25	0.00129	51.5	0.0033
	800	0.044	0.25	0.00129	51.5	0.0034
	1000	0.049	0.26	0.00129	51.5	0.0037
	1200	0.060	0.26	0.00129	51.5	0.0045
Vacuum	400	0.026	0.24	0.00129	51.5	0.0021
	600	0.025	0.25	0.00129	51.5	0.0020
	800	0.027	0.25	0.00129	51.5	0.0021
	1000	0.029	0.26	0.00129	51.5	0.0022
	1200	0.033	0.26	0.00129	51.5	0.0025

VITREOUS SILICA (RTV 60 COATED)

	Temperature (°F)	Avg. Therm. Conductance (Btu/hr ft °F)	Specific Heat (Btu/lb°F)	Thickness Under Load (ft)	Density (lb/ft^3)	Thermal Diffusivity (ft^2/hr)
Ambient Pressure	400	0.066	*	0.001607	*	*
	600	0.063	*	0.001607	*	*
	800	0.061	*	0.001607	*	*
	1000	0.060	*	0.001607	*	*
	1200	0.061	*	0.001607	*	*
Vacuum	400	0.033	*	0.001614	*	*
	600	0.035	*	0.001614	*	*
	800	0.036	*	0.001614	*	*
	1000	0.036	*	0.001614	*	*
	1200	0.037	*	0.001614	*	*

VITREOUS SILICA (PARSON'S OPTICAL BLACK COATED)

	Temperature (°F)	Avg. Therm. Conductance (Btu/hr ft °F)	Specific Heat (Btu/lb°F)	Thickness Under Load (ft)	Density (lb/ft^3)	Thermal Diffusivity (ft^2/hr)
Ambient Pressure	400	0.049	*	0.00241	*	*
	600	0.065	*	0.00241	*	*
	800	0.079	*	0.00241	*	*
	1000	0.089	*	0.00241	*	*
	1200	0.095	*	0.00241	*	*
Vacuum	400	0.028	*	0.00241	*	*
	600	0.035	*	0.00241	*	*
	800	0.042	*	0.00241	*	*
	1000	0.049	*	0.00241	*	*
	1200	0.056	*	0.00241	*	*

RENE 41 (UNCOATED)

	Temperature (°F)	Avg. Therm. Conductance (Btu/hr ft °F)	Specific Heat (Btu/lb°F)	Thickness Under Load (ft)	Density (lb/ft^3)	Thermal Diffusivity (ft^2/hr)
Ambient Pressure	400	0.017	*	0.000248	*	*
	600	0.017	*	0.000248	*	*
	800	0.018	*	0.000248	*	*
	1000	0.023	*	0.000248	*	*
	1200	0.030	*	0.000248	*	*
Vacuum	400	0.012	*	0.000243	*	*
	600	0.011	*	0.000243	*	*
	800	0.012	*	0.000243	*	*
	1000	0.016	*	0.000243	*	*
	1200	0.023	*	0.000243	*	*

RENE 41 (CS105 COATED)

	Temperature (°F)	Avg. Therm. Conductance (Btu/hr ft °F)	Specific Heat (Btu/lb°F)	Thickness Under Load (ft)	Density (lb/ft^3)	Thermal Diffusivity (ft^2/hr)
Ambient Pressure	400	0.041	*	0.000341	*	*
	600	0.044	*	0.000341	*	*
	800	0.049	*	0.000341	*	*
	1000	0.058	*	0.000341	*	*
	1200	0.035	*	0.000341	*	*
Vacuum	400	0.013	*	0.000344	*	*
	600	0.010	*	0.000344	*	*
	800	0.015	*	0.000344	*	*
	1000	0.034	*	0.000344	*	*
	1200	0.023	*	0.000344	*	*

* Information Not Available

Table 2

TOTAL NORMAL TRANSMITTANCE, REFLECTANCE, AND EMITTANCE VALUES

Material	Temperature °F	Transmittance	Reflectance	Emittance	% Total Energy
HT-1 Type I	620	.29	.25	.46	68
	800	.27	.26	.47	77
	990	.31	.28	.41	80
HT-1 Type II	178	.20	.22	.58	25
	400	.20	.22	.58	45
HT-1 Type III	175	.15	.29	.56	24
	400	.13	.31	.56	45
	620	.11	.32	.57	61
1N-Nylon	85	.26	.26	.48	22
	265	.30	.30	.40	45
11N-Nylon	178	.46	.29	.25	26
	400	.46	.33	.21	45
Vitreous Silica Uncoated	620	.15	.30	.55	69
	1165	.16	.36	.48	82
	1800	.28	.46	.26	77
Vitreous Silica R.T.V. 60 Coated	175	.14	.24	.62	24
	400	.15	.20	.65	45
	620	.16	.25	.59	61
Vitreous Silica Parson's Coated	265	.12	.25	.63	24
	620	.06	.17	.77	53
	800	.06	.14	.80	63
Aluminized Fiberglass with Alum. Side Irradiated	175	0	.85	.15	26
	400	0	.74	.26	54
	620	0	.70	.30	68
Aluminized Fiberglass with Non-Alum. Side Irradiated	175	0	.33	.67	26
	400	0	.36	.64	54
	620	0	.39	.61	68
Pluton	265	.30	.32	.38	24
	620	.30	.42	.28	52
	800	.30	.43	.27	62
Fiberglass Al100 Coating	400	.13	.31	.56	54
	990	.16	.41	.43	80
	1530	.17	.44	.39	81
Rene' 41 Uncoated	400	.37	0	.63	45
	800	.39	0	.61	70
	1350	.42	0	.58	79
Rene' 41 CS 105 Coated	400	.17	.29	.54	36
	800	.11	.26	.63	62
	990	.09	.26	.65	69
Stainless Steel	175	.47	.01	.52	32
	400	.45	.01	.54	54
	720	.48	.01	.51	73
Graphite	400	.14	.24	.62	54
	990	.07	.17	.76	80
	1350	.05	.17	.78	82

REFERENCES

1. G. Engholm, R.J. Baschiere, R. A. Bambenek, "Instantaneous Local Temperatures of Aerodynamic Decelerators, Part I, Method of Predicting WADD TR-60-670, Part I, Dec. 1960.

2. G. Engholm, S. J. Lis, R. A. Bambenek, "Instantaneous Local Temperatures of Aerodynamic Decelerators, Part II, Thermal Properties" WADD TR 60-670 Part II, Feb. 1961.

3. Eckert, E. R. G., Heat & Mass Transfer, McGraw-Hill Book Co., Inc. New York, New York, 1959, p. 361-365, 37.

4. Jakob, Max, Heat Transfer, Vol. 1, John Wiley & Sons, Inc., 1949, pp. 24-26.

5. Edwards, D. F., The Emissivity of a Conical Black Body, University of Michigan Engineering Research Institute Report 2144-105-T, Nov. 1959 (Available as ASTIA AD 121838).

6. O'Sullivan, W. J. Jr. & Wade, W. R., Theory & Apparatus for Measurement of Emissivity for Radiative Cooling of Hypersonic Aircraft with Data for Inconel and Inconel X, NACA TN 4121, 1957

7. Clark, C., Vinegar, R.& Hardy, J.D., Goniometric Spectrometer for the Measurement of Diffuse Reflectance & Transmittance of Skin in the Infrared Spectral Region, Jr. of the Optical Society of America, Vol. 43, No. 11, p. 993, November 1953.

8. Dunkle, R. V., Ehrenburg, R., and Gier, J. T., "Spectral Characteristics of Fabrics from 1 to 23 Microns, "Transactions of ASME, Journal of Heat Transfer, February, 1960, pp. 64 to 70.

9. Sanders, C. L. and Middleton, E. E., "The Absolute Spectral Diffuse Reflectance of Magnesium Oxide in the Near Infrared", Journal of Op. Soc. of Am., Vol. 43, No. 1, January, 1953, p. 58.

10. Gier, J. T., Dunkle, R. V. and Bevans, J. T., "Measurement of Absolute Spectral Reflectance from 1.0 to 15 Microns", Journal of Op. Soc. of Am., Vol. 44, No. 7, July 1954, pp. 558 to 562.

GLOSSARY

Emission	is the act or process by which radiant energy is emitted by a body as a consequence of its temperature only. Units of energy per unit area and time. It is influenced by the composition, thickness and surface texture of a specimen.
Emissivity	A theoretical property of a material (independent of any surface effects) defined as a ratio of a rate of emission of radiant energy by an opaque body composed of that material as a consequence of its temperature only, to the corresponding rate for a blackbody at the same temperature. Values can range from 0 to 1.
Emittance	A property of a real body or system at some constant temperature defined as the ratio of a rate of emission of radiant energy by the body in consequence of its temperature only to the corresponding rate for a blackbody at the same temperature. The condition of the surface of the body, polished or not, oxidized or not, and the condition as to opaqueness are immaterial.
Reflectance (or Transmittance)	A property of a body at some constant temperature defined as the ratio of the intensity of the reflected (or transmitted) radiant energy to the intensity of the incident radiant energy. Values can range from 0 to 1.
Hemispherical	refers to energy emitted in all possible directions from a flat surface.
Directional	refers to the energy emitted at a specified angle to the surface.
Normal	refers to the energy emitted in a direction normal to the surface.
Total	refers to the energy emitted at all wavelengths.
Spectral	refers to the energy emitted at specified wavelengths.
Diffuse	refers to energy emitted equally in all directions from a surface.
Specular	refers to energy emitted in preferred directions from a surface.